

LBL-51460



SXNS

The 7th International  
Conference on  
Surface X-Ray and  
Neutron Scattering

Program and Abstracts

September 23–27, 2002  
Granlibakken Conference Center  
Lake Tahoe, California



The 7th International  
Conference on  
Surface X-Ray and  
Neutron Scattering

Program and Abstracts

Co-chairs:

John Ankner, Spallation Neutron Source

Sean Brennan, Stanford Synchrotron Radiation Laboratory

Jeffrey Kortright, Advanced Light Source, Berkeley Lab

September 23–27, 2002

Granlibakken Conference Center

Lake Tahoe, California

## SPONSORS

- Advanced Light Source, Berkeley Lab, Berkeley, CA
- Spallation Neutron Source, Oak Ridge, TN
- Stanford Synchrotron Radiation Laboratory, Stanford, CA
- Blake Industries, Inc., Scotch Plains, NJ
- Neutron Scattering Society of America
- Huber Diffraktionstechnik GmbH, Rimsting, Germany

## ORGANIZATION

### Conference Co-chairs

- John Ankner, Spallation Neutron Source, Oak Ridge, TN, USA
- Sean Brennan, Stanford Synchrotron Radiation Laboratory, Palo Alto, CA, USA
- Jeff Kortright, Advanced Light Source, Berkeley Lab, Berkeley CA, USA

### Program Committee

- Julie Borchers, National Institute of Standards and Technology, Gaithersburg, MD, USA
- Hiroo Hashizume, Nara Institute of Science and Technology (AIST), Nara, Japan
- Ian Robinson, University of Illinois, Urbana, IL, USA
- John White, The Australian National University, Canberra, Australia
- Hartmut Zabel, Ruhr University, Bochum, Germany

### International Advisory Committee

- Jens Als-Nielsen, Niels Bohr Institute, Copenhagen, Denmark
- John Ankner, Spallation Neutron Source, Oak Ridge, TN, USA
- Sean Brennan, Stanford Synchrotron Radiation Laboratory, Stanford, CA, USA
- Helmut Dosch, Max Plank Institute, Stuttgart, Germany
- Gian Felcher, Argonne National Laboratory, Argonne, IL, USA
- Hiroo Hashizume, Nara Institute of Science and Technology (AIST), Nara, Japan
- Jeff Kortright, Lawrence Berkeley National Laboratory, Berkeley, CA, USA
- Hans Lauter, Institut Laue-Langevin, Grenoble, France
- Valeria Lauter-Pasyuk, Institut Laue-Langevin, Grenoble, France
- Gerd Materlik, Diamond Project, Rutherford Appleton Lab, Oxfordshire, England
- Jeff Penfold, Rutherford Appleton Lab, Oxfordshire, England
- Ian Robinson, University of Illinois, Urbana, IL, USA
- Sushil Satija, National Institute of Standards and Technology, Gaithersburg, MD, USA
- Sunil Sinha, University of California, San Diego, CA, USA
- Ad van Well, Interfaculty Reactor Institute, Delft, Netherlands
- Hoydoo You, Argonne National Laboratory, Argonne, IL, USA
- Hartmut Zabel, Ruhr University, Bochum, Germany

## CONFERENCE WEB SITE

<http://sxns.lbl.gov/index.html>



# PROGRAM

## MONDAY, 23 SEPTEMBER 2002

- 3:00–5:00 P.M. Registration  
5:00–6:00 P.M. Welcome reception, Garden Deck  
6:00–7:30 P.M. Dinner, GranHall

### 7:30 P.M.–9:00 P.M.

#### GRANLIBAKKEN CONFERENCE CENTER LAKE—BAY ROOM

##### 1. New Methods — Neutron Spin Echo

- 7:30 P.M. Welcoming Remarks
- 7:40 P.M. 1.1 (Invited) Enhancing neutron reflection experiments using neutron spin echo  
R. Pynn, M. Fitzsimmons, H. Fritsche, J. Major, T. Rekveldt
- 8:20 P.M. 1.2 (Invited) A combination of neutron resonance, spin echo, and reflectometry: a new technique for probing surface and interface order  
J. Major, C. Anderson, H. Dosch, G.P. Felcher, K. Habicht, T. Keller, S.G.E. te Velthuis

## TUESDAY 24 SEPTEMBER

- 7:30–8:30 A.M. Breakfast, GranHall

### 8:30 A.M.–10:10 A.M.

#### GRANLIBAKKEN CONFERENCE CENTER LAKE—BAY ROOM

##### 2. Magnetic Films — I

- 8:30 A.M. 2.1 (Invited) Magnetization reversal in exchange-biased films  
M.R. Fitzsimmons, C. Leighton, J. Nogues, A. Hoffmann, K. Liu, C.F. Majkrzak, J.A. Dura, J.R. Groves, R.W. Springer, P.N. Arendt, V. Leiner, H. Lauter, H. Fritzsche, I.K. Schuller
- 9:10 A.M. 2.2 Twisted ground state in antiferromagnetically coupled multilayers  
H. Lauter, V. Lauter-Pasyuk, B.P. Toperverg, L. Romashev, M. Milyaev, V. Ustinov
- 9:50 A.M. 2.3 (Invited) Tailoring polarized neutron reflectometry for chiral magnetic structures  
K.V. O'Donovan, J.A. Borchers, C.F. Majkrzak, O. Hellwig, E.E. Fullerton
- 10:10–10:40 A.M. Coffee break, Mountain Deck

### 10:40 A.M.–12:40 P.M.

#### GRANLIBAKKEN CONFERENCE CENTER LAKE—BAY ROOM

##### 3. Film Growth and Surface Structure — I

- 10:40 A.M. 3.1 (Invited) In situ x-ray studies of vapor phase epitaxy of  $\text{PbTiO}_3$   
G.B. Stephenson, D.D. Fong, M.V.R. Murty, S.K. Streiffer, J.A. Eastman, O. Auciello, P.H. Fuoss, C. Thompson, A. Munkholm

11:20 A.M.	3.2	The role of vacancies in homoepitaxial crystal growth: x-ray scattering studies of noble metals P.F. Miceli, C.E. Botez, W.C. Elliott, K. Li, E. Lu, E. Conrad, P.W. Stephens
11:40 A.M.	3.3	Grazing incidence scattering techniques to study nano-structured thin films T.H. Metzger
12:00 NOON	3.4	Surface behaviour at the charge density wave transition in NbSe <sub>2</sub> B.M. Murphy, J. Stettner, M. Traving, M. Sprung, I. Grotkopp, M. Mueller, M. Tolan, W. Press
12:20 P.M.	3.5	Diffuse X-ray scatter from Co/Cu multilayers: probing the kinetics of surfactant-assisted growth B.L. Peterson, R.L. White, B.M. Clemens
12:40 P.M.	3.6	Direct determination of the atomic structure of systems with two-dimensional periodicity Y. Yacoby
1:00–1:40 P.M.		Lunch, Garden Deck
1:40–5:00 P.M.		Free time
5:00–6:00 P.M.		Reception, Pavilion
6:00–7:30 P.M.		Dinner, GranHall

**7:30 P.M.–9:30 P.M.**

**GRANLIBAKKEN CONFERENCE CENTER PAVILION**

**4. Scattering from Solids**

- 4.1 Formation of ordered oxygen phases in epitaxial Nb(110) layers  
O. Hellwig, H.W. Becker, H. Zabel
- 4.2 Magnetic polarizations of Cu layers in immediate proximity to ferromagnetic layers  
N. Hosoito, H. Hashizume, T. Ohkochi, G. Srajer, D. Haskel
- 4.3 Cap layer influence on the spin reorientation transition of an ultrathin Co film  
R. Sellmann, J. Hunter Dunn, J. Langer, A. Hahlin, O. Karis, D. Arvanitis, H. Maletta
- 4.4 Energy-dispersive detection of coherent X-ray scattering  
U. Pietsch, T. Panzer, J. Grenzer, A. Pucher
- 4.5 Porous silicon studies using x-ray grazing incidence techniques  
V. Chamard, G. Dolino, P. Bastie, D. Le Bolloc'h, E. Elkaim, C. Ferrero, J.P. Lauriat, F. Rieutord, D. Thiaudiere
- 4.6 Structural and magnetic properties of EuSe/PbSe, EuSe/PbTe, and EuSe/EuTe superlattices grown by molecular beam epitaxy  
R.T. Lechner, T. Schüllli, G. Springholz, G. Bauer, D. Lott, A. Schreyer, H. Clemens, H. Krenn
- 4.7 The study of the structure and exchange coupling of the Py(Ni<sub>80</sub>Fe<sub>20</sub>)/Cr multilayers on sapphire substrates  
K.L. Yu, M.Z. Lin, C.H. Lee, J.C.A. Huang, Z.A. Ku
- 4.8 In situ Neutron Reflection study of the Li intercalation mechanism in thin film anatase TiO<sub>2</sub>  
M. Wagemaker, A.A. van Well

- 4.9 Quasi-in situ reflection mode EXAFS at the Ti/K edge of lithium intercalated rutile and mixed anatase/rutile TiO<sub>2</sub> thin films  
M. Wagemaker, D. Lützenkirchen-Hecht, P. Keil, R. Frahm, A.A. van Well
- 4.10 Influence of x-ray illumination on thin Ti/C films  
K.M. Zimmermann, L. Bruegemann, D. Weissbach, R. Dietsch, M. Tolan
- 4.11 Deuterium in 001-oriented Mo<sub>0.5</sub>V<sub>0.5</sub>/V: the vanishing superlattice  
V. Leiner, H. Zabel, J. Birch, B. Hjörvarsson
- 4.12 The ADAM reflectometer at ILL  
V. Leiner, H. Zabel, M. Wolff
- 4.13 Resonant magnetic scattering of X rays from magnetically rough films in the DWBA\*  
D.R. Lee, S.K. Sinha
- 4.14 Study of surface structural inhomogeneities of the MnO<sub>2</sub> thin films by small-angle x-ray scattering  
L. Skatkov, V. Gomozov
- 4.15 Quantitative determination of the resonant magneto-optical constants at the Gd M<sub>4,5</sub> edges  
J. Miguel, J.F. Peters, O.R.M. Toulemonde, J.B. Goedkoop, S. Dhesi, N.B. Brookes
- 4.16 Spin-polarized neutron reflectivity and magnetization study of Nb/Al multilayers  
S.W. Han, J. Farmer, P.F. Miceli, G.P. Felcher, R. Goyette, G.T. Kiehne, J.B. Ketterson
- 4.17 Magnetism at a buried Co/Pd interface probed by standing-wave enhanced magnetic circular dichroism  
S.K. Kim, J. Kortright
- 4.18 Structure determination of submonatomic Sn layers in Fe/Cr(Sn)Cr magnetic multilayers using anomalous x-ray scattering techniques  
K. Ishiji, H. Okuda, N. Hosoi, H. Hashizume
- 4.19 Structural characterization of ZnO /Al<sub>2</sub>O<sub>3</sub>(11-20) and Au/ZnO/Al<sub>2</sub>O<sub>3</sub>(11-20) films by x-ray scattering  
M. Ay, A. Nefedov, H. Zabel
- 4.20 Improved compact x-ray sources  
A. Mozelev

## WEDNESDAY, 25 SEPTEMBER 2002

7:30–8:30 A.M. Breakfast, GranHall

**8:30 A.M.–10:30 A.M.**

**GRANLIBAKKEN CONFERENCE CENTER LAKE—BAY ROOM**

### 5. Film Growth and Surface Structure — II

- 8:30 A.M. 5.1 (Invited) Use of coherent x-ray diffraction to image surface structure  
I.K. Robinson
- 9:10 A.M. 5.2 X-ray scattering measurements of concentration enhanced interdiffusion at Si/SiGe interfaces  
D.B. Aubertine, N. Ozguven, A.F. Marshall, P.C. McIntyre
- 9:30 A.M. 5.3 Grazing incidence small angle x-ray scattering for measuring particle/pore-size distributions in thin films  
K. Omote, Y. Ito, K. Inaba

- 9:50 A.M. 5.4 Vertical alignment of GaN quantum dots stacked in multilayers: correlation length, depth-resolved strain analysis, and elastic energy distribution  
V. Chamard, T.H. Metzger, V. Holý, M. Sztucki, M. Tolan, E. Bellet-Amalric, B. Daudin, C. Adelmann, H. Mariette
- 10:10 A.M. 5.5 Determination of absolute indium content in InGaN/GaN multiple quantum wells using anomalous x-ray scattering  
D.Y. Noh, H.H. Lee, K.S. Liang
- 10:30–11:00 A.M. Coffee break, Mountain Deck

**11:00 A.M.–1:00 P.M.**

**GRANLIBAKKEN CONFERENCE CENTER LAKE—BAY ROOM**

**6. Soft X Rays**

- 11:00 A.M. 6.1 (Invited) Magnetic x-ray scattering as a probe of heterogeneous magnetic thin films  
E.E. Fullerton
- 11:40 A.M. 6.2 Resonant small-angle x-ray scattering of polymers at the Carbon K edge  
I. Koprinarov, G. Mitchell, B. Landes, J. Lyons, B. Kern, M. Devon, J.B. Kortright
- 12:00 NOON 6.3 Detailed study of magnetic reversal in stripe domain systems using Resonant X-ray Magnetic Scattering  
J.F. Peters, J. Miguel, O.R.M. Toulemonde, J.B. Goedkoop, S. Dhesi, N.B. Brookes
- 12:20 P.M. 6.4 Probing thin film magnetic domain structures by resonant soft x-ray small angle scattering  
O. Hellwig, J.B. Kortright, E.E. Fullerton
- 12:40 P.M. 6.5 Magnetic x-ray reflectivity study of an Fe/Cr multilayer  
D. Lott, C.C. Kao, C. Sanchez-Hanke, G.P. Felcher, J.S. Jiang, S.D. Bader
- 1:00–2:00 P.M. Lunch, Garden Deck
- 2:00–5:00 P.M. Free time
- 5:00–6:00 P.M. Reception, Pavilion
- 6:00–7:30 P.M. Dinner, GranHall

**7:30 P.M.–9:30 P.M.**

**GRANLIBAKKEN CONFERENCE CENTER PAVILION**

**7. Scattering from Soft Matter and Liquids**

- 7.1 Interaction of the antimicrobial frog peptide, PGLa, with lipid monolayers studied by X-ray grazing incidence diffraction and reflectivity  
O. Konovalov, K. Lohner, I. Myagkov, B. Struth
- 7.2 Growth control of organic thin films  
B. Nickel, L. Casalis, M.F. Danisman, G. Scoles, S. Ianotta, R. Ruiz
- 7.3 Neutron Reflection from the Liquid/Liquid Interface  
J. Webster, A. Zarbakhsh, J. Bowers
- 7.4 Model lung surfactant lipid monolayers and the influence of pulmonary surfactant B on the lipid phase behaviour  
F. Bringezu, G. Brezesinski, J.A. Zasadzinski, J. Ding, A. Waring
- 7.5 X-ray Scattering Studies on InGaAs Quantum Dots  
C.-H. Hsu, Y.P. Stetsko, H.Y. Lee, N.T. Yeh, J.-I. Chyi, D.Y. Noh, M.T. Tang, K.S. Liang

- 7.6 Investigation of confined and thin film polymers using x-ray scattering methods  
O.H. Seeck, M. Mihaylova, H. Kim, S.K. Sinha, D. Lambreva, Y. Serero, W. deJeu
- 7.7 X-ray scattering at metal/polymer interfaces  
R. Weber, I. Grotkopp, V. Chamard, J. Stettner, W. Press, M. Tolan, O.H. Seeck
- 7.8 Generic phase behavior of branched-chain phospholipid monolayers  
G. Brezesinski, F. Bringezu
- 7.9 Neutron reflectivity applied to DNA chips  
F. Cousin, A. Menelle, F. Boué
- 7.10 Hydrogen as a tuning agent of the interlayer exchange coupling  
V. Leiner, K. Westerholt, H. Zabel, B. Hjörvarsson
- 7.11 Real-Time In-Plane Diffusion of Au Nanoparticles in Polymer Thin Films  
S. Narayanan, R. Guico, D.R. Lee, J. Wang, A. Gibaud, S.K. Sinha
- 7.12 Neutron reflection study on the lipophilic-C60 derivative at the air/water interface  
U.S. Jeng, T.L. Lin, Z.-M. Lin, Z.A. Chi, .M.C. Shih, L.Y. Chiang, K. Shin
- 7.13 SANS studies of polyelectrolyte multilayers on colloids and hollow capsules  
I. Estrela-Lopis, S. Leporatti, E. Donath
- 7.14 Design and estimated performance of the SNS liquids reflectometer  
J.F. Ankner, Ch. Rehm, R.L. Kellogg
- 7.15 SNS: The next generation neutron source  
J.F. Ankner (presenting author) and The SNS Instrument Systems Group
- 7.16 Liquid surface/interface spectrometer at ChemMatCARS Synchrotron Facility at the Advanced Photon Sources  
B. Lin, M. Meron, J. Gebhardt, T. Graber, P.J. Viccaro, M. Schlossman

## THURSDAY, 26 SEPTEMBER 2002

7:30–8:30 A.M. BREAKFAST, GRANHALL

**8:30 A.M.–10:30 A.M.**

**GRANLIBAKKEN CONFERENCE CENTER LAKE—BAY ROOM**

### 8. Liquids and Soft Matter — I

- 8:30 A.M. 8.1 (Invited) high-energy X rays for the study of solid/liquid Interfaces  
H. Reichert
- 9:10 A.M. 8.2 Capillary waves on water  
C. Gutt, M. Tolan, T. Ghaderi, A. Madsen, T. Seydel, V. Chamard
- 9:30 A.M. 8.3 X-ray photon correlation spectroscopy on polymer films with molecular weight dependence  
H. Kim, A. Rühm, L. Lurio, J. Basu, J. Lal, S. Mochrie, S.K. Sinha
- 9:50 A.M. 8.4 Real time measurements of nanoparticle diffusion in ultrathin polymer films using x-ray standing waves  
R.S. Guico, S. Narayanan, J. Wang, K. Shull

10:10 A.M. 8.5 Lipid discrimination of antimicrobial peptides studied by GIXD  
F. Bringezu, G. Brezesinski, A. Waring, R.I. Lehrer

10:30–11:00 A.M. Coffee break, Mountain Deck

**11:00 A.M.–1:00 P.M.**

**GRANLIBAKKEN CONFERENCE CENTER LAKE—BAY ROOM**

**9. Liquids and Soft Matter — II**

- 11:00 A.M. 9.1 (Invited) Surface dynamics of polymer films studied via XPCS  
S.G.J. Mochrie, H. Kim, S.K. Sinha, J. Lal, J. Basu, A. Ruehm, L.B. Lurio
- 11:40 A.M. 9.2 Dynamics of a liquid crystal surface near the Nematic-to-Smectic A  
transition: A critical scattering study applying coherent X rays  
A. Madsen, G. Grübel, J. Als-Nielsen
- 12:00 NOON 9.3 X-ray and neutron surface investigations of highly viscous liquids  
T. Seydel, A. Madsen, M. Tolan, B.M. Ocko, J. Major
- 12:20 P.M. 9.4 (Invited) Thin-film polymers used as x-ray waveguides  
T. Salditt
- 1:00–2:00 P.M. Lunch, Garden Deck
- 2:00–5:00 P.M. Free time
- 5:00–6:00 P.M. Reception
- 6:00–7:30 P.M. Dinner, GranHall

**7:30 P.M.–9:30 P.M.**

**GRANLIBAKKEN CONFERENCE CENTER LAKE—BAY ROOM**

**10. Magnetic Films — II**

- 7:30 P.M. 10.1 (Invited) Supermatrix formalism to model off-specular neutron scattering  
B.P. Toperverg
- 8:10 P.M. 10.2 (Invited) Mapping magnetic disorder in magnetic multilayers  
S. Langridge, R.M. Dalgliesh, C.H. Marrows, B.J. Hickey, M. Ali, A.T. Hindmarch
- 8:50 P.M. 10.3 Polarized neutron reflectivity studies on laterally structured stripe arrays  
K. Theis-Bröhl, V. Leiner, T. Schmitte, H. Zabel
- 9:10 P.M. 10.4 Self-assembled nanomaterials: magnetic nanoparticles in copolymer films  
studied by off-specular neutron scattering  
V. Lauter-Pasyuk, H. Lauter, G. Gordeev, P. Müller-Buschbaum, B.P. Toperverg, W.  
Petry

## FRIDAY, 27 SEPTEMBER 2002

7:30–8:30 Breakfast, GranHall

### 8:30 A.M.–10:10 A.M.

#### GRANLIBAKKEN CONFERENCE CENTER LAKE—BAY ROOM

##### 11. Liquids and Soft Matter — III

- 8:30 A.M. 11.1 X-ray and neutron surface studies of cholera toxins interaction with lipid monolayer at the air/water interface  
J. Majewski, T. Kuhl, G. Smith, K. Kjaer, S. Satija
- 8:50 A.M. 11.2 Structure of brushite/water interface  
J. Arsic, D. Kaminski, P. Poodt, E. Vlieg
- 9:10 A.M. 11.3 In situ x-ray standing wave profiling of biomolecular adsorption at a charged interface  
M.J. Bedzyk, K. Zhang, J. Libera, H. Cheng, M. Olvera de la Cruz, L. Cao
- 9:30 A.M. 11.4 Thermal denaturation of interfacial protein layers  
J.W. White, M.J. Henderson, S.A. Holt
- 9:50 A.M. 11.5 X-ray and neutron scattering studies of mesoporous silicate films  
S.A. Holt, J.L. Ruggles, J.W. White
- 10:10–10:40 A.M. Coffee break, Mountain Deck

### 10:40 A.M.–12:10 P.M.

#### GRANLIBAKKEN CONFERENCE CENTER LAKE—BAY ROOM

##### 12. New Methods — Direct Inversion

- 10:40 A.M. 12.1 (Invited) Solving the inverse problem of surface x-ray diffraction  
D.K. Saldin
- 11:20 A.M. 12.2 (Invited) Phase Determination and Direct Inversion in Specular Neutron Reflectometry  
C. Majkrzak, N.F. Berk
- 12:00–12:10 P.M. Closing remarks
- 12:10–1:10 P.M. Lunch, Garden Deck
- 1:10 P.M. Adjourn



# **ABSTRACTS**



**SESSION NO. 1, 7:30 PM**  
**Monday, 23 September 2002**  
**NEW METHODS — NEUTRON SPIN ECHO**  
**GRANLIBAKKEN CONFERENCE CENTER LAKE-BAY ROOM**

**1.1. Enhancing neutron reflection experiments using neutron spin echo (Invited)**

R. Pynn,<sup>1\*</sup> M. Fitzsimmons,<sup>1</sup> H. Fritsche,<sup>2</sup> J. Major,<sup>3</sup> T. Rekveldt<sup>4</sup>

<sup>1</sup>Los Alamos National Laboratory, USA, <sup>2</sup>Hahn-Meitner Institute, Germany, <sup>3</sup>Max-Planck-Institut für Metallforschung, Germany, <sup>4</sup>Delft University of Technology, Netherlands

E-mail: [pynn@mrl.ucsb.edu](mailto:pynn@mrl.ucsb.edu)

For most surface reflection experiments, x-rays provide both better resolution and greater statistical precision than neutrons. Neutrons are preferred only in situations in which their sensitivity to isotopic contrast and magnetism, or their ability to penetrate thick layers of material, can be exploited. Even in these cases, special techniques are often needed to achieve sufficient signal intensity at acceptable resolution. In this contribution, we present one such technique, based on neutron spin echo, that appears to offer several promising enhancements. The technique should allow specular neutron reflection to be measured with high intensity and with negligible contamination from diffuse scattering, even in cases where the incident neutron beam has a broad angular divergence. In addition, the method is expected to allow structure within the plane of a reflecting sample to be monitored with good spatial resolution. Finally, it may allow a unique aspect of neutron scattering—its ability to measure inelastic scattering—to be exploited in surface scattering experiments.

\* Present address: Materials Research Laboratory, University of California at Santa Barbara, Santa Barbara, California, 93103.

**1.2. A combination of neutron resonance, spin echo, and reflectometry: a new technique for probing surface and interface order (Invited)**

J. Major,<sup>1</sup> C. Anderson,<sup>1</sup> H. Dosch,<sup>1</sup> G.P. Felcher,<sup>2</sup> K. Habicht,<sup>3</sup> T. Keller,<sup>4</sup> S.G.E. te Velthuis<sup>2</sup>

<sup>1</sup>Max-Planck-Institut für Metallforschung, Germany, <sup>2</sup>Argonne National Laboratory, USA,

<sup>3</sup>Hahn-Meitner-Institut, Germany, <sup>4</sup>Max-Planck-Institut für Festkörperforschung, Germany

E-mail: [major@mf.mpg.de](mailto:major@mf.mpg.de)

In neutron reflectometry experiments, in which the scattering is not dependent on the neutron spin, the application of the neutron spin echo (NSE) technique opens a way for the determination of the out-of-scattering-plane scattering angle without the use of additional slits, i.e., with a loss in intensity of only 50%. Although the basic idea is nearly as old as the NSE itself, its realization became feasible only recently when new experimental possibilities were developed, such as the neutron resonance spin echo (NRSE) technique. In our talk, we will present the design of a spin-echo resolved grazing incidence scattering (SERGIS) setup, i.e., a neutron reflectometer with an NRSE extension. Such an instrument will also give easy access to inelastic grazing-incidence scattering.

\* \* \*

**SESSION NO. 2, 8:30 AM**  
**TUESDAY, 24 SEPTEMBER 2002**  
**MAGNETIC FILMS — I**  
**GRANLIBAKKEN CONFERENCE CENTER LAKE-BAY ROOM**

**2.1. Magnetization reversal in exchange-biased films (Invited)**

M.R. Fitzsimmons,<sup>1</sup> C. Leighton,<sup>2</sup> J. Nogues,<sup>3</sup> A. Hoffmann,<sup>4</sup> K. Liu,<sup>5</sup> C.F. Majkrzak,<sup>6</sup> J.A. Dura,<sup>6</sup> J.R. Groves,<sup>1</sup> R.W. Springer,<sup>1</sup> P.N. Arendt,<sup>1</sup> V. Leiner,<sup>7</sup> H. Lauter,<sup>7</sup> H. Fritzsche,<sup>8</sup> I.K. Schuller<sup>9</sup>

<sup>1</sup>Los Alamos National Laboratory, USA, <sup>2</sup>University of Minnesota, <sup>3</sup>Institucio Catalana de Recerca i Estudis Avancats and Department de Fisica, <sup>4</sup>Argonne National Laboratory, <sup>5</sup>University of California at Davis, <sup>6</sup>National Institute of Standards and Technology, <sup>7</sup>Institute Laue Langevin, <sup>8</sup>Hahn-Meitner Institute, <sup>9</sup>University of California at San Diego

E-mail: [fitz@lanl.gov](mailto:fitz@lanl.gov)

Polarized neutron reflectometry was used to determine the anisotropies of polycrystalline ferromagnetic (F) Fe thin films exchange coupled to antiferromagnetic (AF) untwinned single crystal (110) FeF<sub>2</sub>, twinned single crystal (110) FeF<sub>2</sub> thin films and (110) textured polycrystalline FeF<sub>2</sub> thin films. A correlation between the anisotropies of the AF and F thin films with exchange bias was identified. For the AF single crystal sample, we observed perpendicular exchange coupling across the F/AF interface, which is manifested by symmetric production of neutron spin-flip scattering on either side of the hysteresis loop at coercivity. Perpendicular exchange coupling was observed regardless of cooling field orientation, even though exchange bias was clearly affected by the cooling field orientation; thus, perpendicular exchange coupling is not a sufficient condition for exchange bias. For twinned AF samples, an asymmetry in the spin-flip scattering on either side of the hysteresis loop, and consequently in the magnetization reversal process, was observed. The origin of the asymmetry is shown to be frustration of the perpendicular exchange coupling, which enhances exchange bias and leads to 45° exchange coupling across the F-AF interface. Specifically, when exchange coupling across the F-AF interface introduces an additional anisotropy axis in the F thin film—one perpendicular to the cooling field, the magnetization reversal mechanism, is affected and exchange bias is significantly enhanced.

This work is supported by the U.S. Department of Energy, BES-DMS, under Contract No. W-7405-Eng-36, and Grant No. DE-FG03-87ER-45332.

## 2.2. Twisted ground state in antiferromagnetically coupled multilayers

H. Lauter,<sup>1</sup> V. Lauter-Pasyuk,<sup>2</sup> B.P. Toperverg,<sup>3</sup> L. Romashev,<sup>4</sup> M. Milyaev,<sup>4</sup> V. Ustinov<sup>4</sup>

<sup>1</sup>Institute Laue Langevin, France, <sup>2</sup>TU München c/o ILL, France, <sup>3</sup>FZ Jülich, Germany, <sup>4</sup>IMP, Russia  
E-mail: [lauter@ill.fr](mailto:lauter@ill.fr)

The complete two-dimensional analysis of specular reflection and off-specular scattering with polarized neutrons gives uniquely detailed information on the lateral and transverse spin-configuration of a multilayer (ML) stack. We present the direct experimental observation of a phenomenon existing in antiferromagnetically coupled ML: the twisted ground-state configuration in an external magnetic field. It is shown that in finite superlattices the presence of two surfaces influences the configuration of magnetic moments through the entire ML. This fact can be already established just via the qualitative analysis of the line shape of the superstructure peaks on the specular line and the related off-specular Bragg-sheet position.

The qualitative data analysis used a formalism based on the Distorted Wave Born Approximation. It was found that the canting angles determined by the layer magnetic moment directions of the  $[^{57}\text{Fe}/\text{Cr}]_n$  ML are maximal in the end layers and progressively relax towards the middle of the ML from both sides. The magnetic moments in the two end layers are tilted in antiphase for an even number of magnetic layers. The presence of spin-flip off-specular scattering means that the layer magnetization is laterally not homogeneous but is decomposed into a set of domains. The distribution of magnetic moments within each domain, as well as the domain's sizes and distributions, are obtained.

The angular distribution of layer magnetic moments as a function of the magnetic field including the surface spin-flop is discussed.

## 2.3. Tailoring polarized neutron reflectometry for chiral magnetic structures (Invited)

K.V. O'Donovan,<sup>1</sup> J.A. Borchers,<sup>1</sup> C.F. Majkrzak,<sup>1</sup> O. Hellwig,<sup>2</sup> E.E. Fullerton<sup>2</sup>

<sup>1</sup>National Institute of Standards and Technology, USA, <sup>2</sup>IBM Almaden Research Center, USA  
E-mail: [kevin.odonovan@nist.gov](mailto:kevin.odonovan@nist.gov)

The twists of Bloch domain walls may be the driving mechanism behind such phenomena as exchange biasing and exchange-spring magnets, and the ability to track their development in magnetic fields should help resolve why some of these materials do not behave as expected from current theories. We used spin-polarized neutron reflectometry (PNR) to study the spin structure of an FePt|NiFe exchange-coupled magnetic bilayer in magnetic field and in remanence. We applied our recently developed technique, which improves the sensitivity of PNR, to buried magnetic twists. The implementation is straightforward: the neutron reflectivity is measured with neutrons scattering from the back surface as well as the front surface, thus yielding eight spin cross-sections instead of the usual four. Our technique quickly identifies the noncollinear magnetism accompanying buried twists, regardless of the presence of chiral domains of clockwise and anticlockwise twists. We have characterized the spin structure of the exchange spring as a function of field, both applied and remanent. We shall discuss the advantages of our PNR technique and the sorts of magnetic structures that benefit most from its use.

\* \* \*

**SESSION No. 3, 10:40 AM**  
**TUESDAY, 24 SEPTEMBER 2002**  
**FILM GROWTH AND SURFACE STRUCTURE — I**  
**GRANLIBAKKEN CONFERENCE CENTER LAKE-BAY ROOM**

**3.1. In situ x-ray studies of vapor phase epitaxy of PbTiO<sub>3</sub> (Invited)**

G.B. Stephenson,<sup>1</sup> D.D. Fong,<sup>1</sup> M.V.R. Murty,<sup>1</sup> S.K. Streiffer,<sup>1</sup> J.A. Eastman,<sup>1</sup> O. Auciello,<sup>1</sup> P.H. Fuoss,<sup>1</sup>  
C. Thompson,<sup>2</sup> A. Munkholm<sup>3</sup>

<sup>1</sup>Argonne National Laboratory, USA, <sup>2</sup>Northern Illinois University, USA, <sup>3</sup>Lumileds Lighting, USA  
E-mail: [stephenson@anl.gov](mailto:stephenson@anl.gov)

As part of a program to understand and control the structure of ferroelectric thin films grown by metal organic vapor phase epitaxy (MOVPE), we have been using x-ray scattering to observe the surface structure of PbTiO<sub>3</sub> films during and following growth. We use moderately high energy (24 keV) x-rays to penetrate the chamber walls for in situ measurements in the high-temperature, reactive MOVPE environment. Performing measurements in situ allows us to study the growth process in real time, to control the thickness of the films to sub-unit-cell accuracy, to observe the surface structure in equilibrium with the vapor, and to preserve film stoichiometry during high-temperature study by maintaining an overpressure of PbO. While the higher x-ray energy also allows a large volume of reciprocal space to be mapped, it presents challenges for surface scattering due to the small critical angle. Examples of results will be presented from studies of equilibrium surface structure [1], dynamics of surface phase transitions and crystal growth [2], and surface effects on ferroelectricity in thin films determined by coherent Bragg rod analysis (COBRA). These experiments were carried out using the BESSRC beamlines at the Advanced Photon Source.

This work is supported by the U.S. Department of Energy under Contract No. W-31-109-ENG-38, and the State of Illinois under HECA.

[1] A. Munkholm et al., Phys. Rev. Lett. 88, 016101 (2002).

[2] M.V. Ramana Murty et al., Appl. Phys. Lett. 80, 1809 (2002).

### 3.2. The role of vacancies in homoepitaxial crystal growth: X-ray scattering studies of noble metals

P.F. Miceli,<sup>1</sup> C.E. Botez,<sup>1</sup> W.C. Elliott,<sup>1</sup> K. Li,<sup>1</sup> E. Lu,<sup>1</sup> E. Conrad,<sup>2</sup> P.W. Stephens<sup>3</sup>

<sup>1</sup>University of Missouri-Columbia, USA, <sup>2</sup>Georgia Institute of Technology, USA, <sup>3</sup>SUNY at Stony Brook, USA

E-mail: [micelip@missouri.edu](mailto:micelip@missouri.edu)

Although there has been considerable recent progress in simulations of epitaxial crystal growth, the accuracy of these simulations is limited to the kinetic mechanisms that are included. This talk will suggest that vacancy formation is ubiquitous for the low-temperature homoepitaxial growth of metals and that the consideration of vacancies is expected to be integrally important to a realistic description of epitaxial crystal growth. X-ray scattering experiments, which reveal the surface morphology simultaneously with the subsurface structure, observe the incorporation of vacancies within the growing film for low-temperature homoepitaxy on Ag(001), Cu(001), and Ag(111). We have measured the temperature dependence of vacancy formation for both (001) systems as well as performed annealing experiments for Cu(001), which gives results that are consistent with the known annealing behavior in radiation damage studies of bulk Cu. Moreover, we observe that the growing surface of Ag(111) undergoes substantial changes concomitantly with the formation of vacancies. Instead of the usual Gaussian distribution of exposed terraces, it is bimodal, reflecting the pyramidal surface morphology combined with a latent memory of the original substrate and, thereby, leading to a surface roughness exponent,  $\beta = 1$ . Reentrant growth, which occurs on the (001) surfaces, will also be discussed in terms of these results.

Funding is acknowledged from the NSF, (PFM) DMR9623827, (PWS) 9202528; and DOE, (PFM) MISCN DOE DE-FGG02-90ER45427 and the Univ. of Missouri Res. Board. Beamline funding: SUNY X3 at NSLS: DOE DE-FG02-86ER4523; APS: DOE W-31-109-Eng-38, and MUCAT through Ames Lab DOE W-7405-Eng-82.

### 3.3. Grazing incidence scattering techniques to study nano-structured thin films

T.H. Metzger, ESRF, France

E-mail: [metzger@esrf.fr](mailto:metzger@esrf.fr)

We have developed x-ray scattering techniques at grazing incidence to analyse the properties of nano-structured thin films on substrates, i.e., semiconductor quantum dots. The morphology and the ordering of the dots are characterised in grazing incidence small-angle scattering (GISAXS). Using grazing incidence diffraction (GID), the crystalline properties of the dots (such as strain, shape, composition, and ordering) are quantified. Results on different semiconductor systems will be presented, demonstrating the versatility of the methods, which can be applied to free-standing and buried dots.

By applying GISAXS to Ge islands grown on boron-terminated Si(111), we can find the shape and size-distribution of nearly perfect triangular pyramids, incoherently connected to the substrate.

An "iso-strain-scattering" technique has been developed in the GID geometry to determine the lattice parameter distribution and the chemical composition in dots. For free-standing InAs dots, the lattice parameter ranges from GaAs at the foot to InAs at the top of the dots. Clear evidence for Ga inter-diffusion into the dots is found.

For QD embedded in multilayers, strong spatial correlations are expected. In the system GaN/AlN QD multilayer, the vertical stacking of the GaN QD was quantified from the analysis of Bragg sheets in the GISAXS region. First results on the use of anomalous diffraction in QD systems will be presented.

### 3.4. Surface behaviour at the charge density wave transition in NbSe<sub>2</sub>

B.M. Murphy,<sup>1</sup> J. Stettner,<sup>1</sup> M. Traving,<sup>1</sup> M. Sprung,<sup>1</sup> I. Grotkopp,<sup>1</sup> M. Mueller,<sup>1</sup> M. Tolan,<sup>2</sup> W. Press<sup>3</sup>

<sup>1</sup>Christian-Albrechts-University, Kiel, Germany, <sup>2</sup>Univ. Dortmund, Germany, <sup>3</sup>Institut Laue-Langevin, France

E-mail: [murphy@physik.uni-kiel.de](mailto:murphy@physik.uni-kiel.de)

The van der Waals bonded layered structure 2H–NbSe<sub>2</sub> undergoes a charge density wave (CDW) transition at 33 K. The complex quantity, which represents the CDW amplitude and phase, may be taken as the order parameter for the phase transition. Therefore, we can study the nature of the phase transition by following the temperature-dependent behaviour of the CDW structure.

We have investigated the CDW transition in NbSe<sub>2</sub> using grazing incidence diffraction. The evolution of the satellite reflection has been observed both at the surface and in the bulk in order to extract the critical exponents and thereby carry out a direct comparison between the surface and bulk behaviour. Within the precision of previous experiments, bulk 2H–NbSe<sub>2</sub> undergoes a second-order phase transition. We successfully isolated the surface CDW structure on a high-quality single crystal using grazing incidence diffraction, at BW2, HASYLAB. The central finding is that the surface CDW satellite differs from that in the bulk: at the surface, the CDW transition temperature is above the bulk transition temperature; also, the transition appears to be continuous. Given that the surface transition occurs before the bulk, it is likely that we observe the unusual case defined as a “surface transition” and related phenomena.

### 3.5. Diffuse x-ray scatter from Co/Cu multilayers: Probing the kinetics of surfactant-assisted growth

B.L. Peterson, R.L. White, B.M. Clemens, Stanford University, USA

E-mail: [brennan.peterson@stanford.edu](mailto:brennan.peterson@stanford.edu)

Surfactants, surface contaminants that change surface kinetics, provide a useful additional tool for controlling the growth of thin films. While their efficacy in improving magnetic films is well established, the attendant structural changes remain unclear. The difficulty derives partly from the varying materials and deposition methods used, and partly from the very low Z-contrast between Co and Cu. Low-angle diffuse scatter investigations clarify the structural details of the films, and tuning the x-ray wavelength to the absorption edge allows both better error correction and enhanced scattering contrast. O<sub>2</sub>, Ag, Pb, and In were investigated as surfactants in the growth of Co/Cu multilayers. DC magnetron sputtered Co/Cu multilayers were deposited on native SiO<sub>2</sub>. O<sub>2</sub> was introduced during growth at partial pressures ranging from 10<sup>-6</sup> to 10<sup>-9</sup> Torr, as well as “puffed” onto interfaces between the two materials. Metallic surfactants were added as either “seed” layers at the base of the multilayer, or at various interfaces within the stack. X-ray scans were taken along the specular (q<sub>z</sub>) direction, perpendicular to the specular (q<sub>x</sub>), as well as offset from the specular condition, in the q<sub>z</sub> direction.

Both oxygen and silver increased the roughness correlation and overall smoothness of the multilayer. Lead and indium were found to decorrelate the layers, while also smoothing the films. This can be explained in the very different kinetic changes caused by the surfactants.

Finally, the application of surfactants to spin valve structures, and the limitations of the technique in analyzing complex multilayers, are discussed.

### 3.6. Direct determination of the atomic structure of systems with two-dimensional periodicity

Y. Yacoby, Racah Institute of Physics, Hebrew University, Jerusalem, Israel

E-mail: [yizhak@vms.huji.ac.il](mailto:yizhak@vms.huji.ac.il)

We present a new method for the measurement of the electron density of systems with two-dimensional periodicity. The method is based on the measurement of the x-ray diffraction intensities along the system Bragg rods, the calculation of the diffraction phase along the Bragg rods, and the subsequent Fourier transformation of the resulting complex scattering factors into real space. We have used this method to obtain the three-dimensional electron density and atomic structure of a  $\text{Gd}_2\text{O}_3$  film grown epitaxially on a GaAs substrate. The results show that the stacking order of the  $\text{Gd}_2\text{O}_3$  film layers is different from that of cubic bulk  $\text{Gd}_2\text{O}_3$  and resembles the stacking order of Ga and As layers in GaAs. Furthermore, in the first few  $\text{Gd}_2\text{O}_3$  layers, Gd atoms are displaced to positions right above the Ga and As positions in the substrate and they relax towards bulk  $\text{Gd}_2\text{O}_3$  positions with increasing distance from the interface.

\* \* \*

**SESSION NO. 4, 7:30 PM**  
**TUESDAY, 24 SEPTEMBER 2002**  
**SCATTERING FROM SOLIDS**  
**GRANLIBAKKEN CONFERENCE CENTER PAVILION**

**4.1. Formation of ordered oxygen phases in epitaxial Nb(110) layers**

O. Hellwig,<sup>1</sup> H.W. Becker,<sup>2</sup> and H. Zabel,<sup>3</sup>

<sup>1</sup>IBM Almaden Research Center, USA, <sup>2</sup>Institut fuer Experimentalphysik/ Ionenstrahlenphysik, Ruhr Universitaet Bochum, Germany, <sup>3</sup>Institut fuer Experimentalphysik/ Festkoerperphysik, Ruhr Universitaet Bochum, Germany

E-mail: [olav@us.ibm.com](mailto:olav@us.ibm.com)

Synchrotron x-ray diffraction studies during the atmospheric oxidation of epitaxial Nb(110) thin films at elevated temperatures reveal the formation of highly ordered oxygen phases within the Nb lattice. The oxygen is stored on interstitial lattice sites leading to an out-of-plane expansion of up to 4.3% without destroying the basic structure of the Nb host lattice. During the oxidation process of a 500 nm Nb layer, we observe the formation of a nonordered lattice gas phase succeeded by a well-defined sequence of oxygen superstructures. Further oxygen incorporation into the system continues until finally the whole film is transformed into amorphous Nb<sub>2</sub>O<sub>5</sub>. By exploiting the high brilliance of synchrotron radiation, it becomes possible to identify the different states of ordered oxygen within the Nb host lattice. With ongoing oxidation the increasing oxygen concentration forces the system to rearrange the oxygen several times. Each ordered oxygen phase can be identified via x-ray diffraction by a specific Nb lattice expansion as well as a characteristic superstructure pattern. Measurements were performed at the W1 beamline at the HASYLAB in Hamburg, Germany.

**4.2. Magnetic polarizations of Cu layers in immediate proximity to ferromagnetic layers**

N. Hosoito,<sup>1</sup> H. Hashizume,<sup>1</sup> T. Ohkochi,<sup>2</sup> G. Srajer,<sup>3</sup> D. Haskel<sup>3</sup>

<sup>1</sup>Nara Institute of Science and Technology, Japan, <sup>2</sup>Kyoto Univ., Japan, <sup>3</sup>Argonne National Laboratory, USA

E-mail: [hosoito@ms.aist-nara.ac.jp](mailto:hosoito@ms.aist-nara.ac.jp)

Antiferromagnetic coupling of ferromagnetic layers in giant magnetoresistance (GMR) multilayer films is mediated by nonmagnetic spacer layers. Magnetic polarizations of Cu layers in Co/Cu multilayers were evidenced by the small but definite x-ray magnetic circular dichroic (XMCD) absorption signals observed by two groups (Phys. Rev. Lett. 72, 1112, 1994; Phys. Rev. Lett. 74, 1470, 1995). We have observed similar but much larger Cu signals from Gd/Cu multilayers at low temperatures. At 10 K, the XMCD signal from a Gd(6 nm)/Cu(2 nm) multilayer peaks slightly above the Cu *K* edge, with a height of  $-0.18\%$  in  $\Delta\mu t$  normalized to the  $\mu t$  jump height, which is about five times as large as the one observed from a Co(1 nm)/Cu(2 nm) multilayer. Interestingly, the main Cu *K* edge XMCD peaks have opposite signs in the Gd/Co and the Co/Cu multilayers, suggesting that the Cu 4p moments are oriented in the opposite directions in the two materials when the Gd 4f moments and the Co 3d moments are aligned along an external in-plane field. In addition, the XMCD spectrum from the Gd/Cu multilayer features large positive subpeaks before and after the main peak. The Gd layers have magnetizations close to the full magnetization of Gd at 10 K, which reduce as temperature is raised towards the Curie temperature, located at 100–150 K in our samples. The Gd/Cu system is a good sample for exploration of the depth profiles of the Cu polarizations by resonant x-ray magnetic specular reflectivity measurements [1]. Even though the Gd/Cu system does not show the GMR effect, this material would provide key information to better understand the mechanism responsible for the interlayer magnetic coupling in GMR films.

[1] N. Ishimatsu, H. Hashizume et al., Phys. Rev. B 60, 9596 (1999).

### 4.3. Cap layer influence on the spin reorientation transition of an ultrathin Co film

R. Sellmann,<sup>1</sup> J. Hunter Dunn,<sup>2</sup> J. Langer,<sup>1</sup> A. Hahlin,<sup>3</sup> O. Karis,<sup>3</sup> D. Arvanitis,<sup>3</sup> H. Maletta<sup>1</sup>

<sup>1</sup>Hahn-Meitner-Institut Berlin, Germany, <sup>2</sup>Stanford Synchrotron Radiation Lab, <sup>3</sup>University of Uppsala, Sweden

E-mail: [maletta@hmi.de](mailto:maletta@hmi.de)

Ultrathin films with dominant perpendicular magnetic anisotropy exhibit a spontaneous out-of-plane magnetization that rotates into the plane with an increase in temperature or film thickness. We have studied systematically the influence of a cap layer on this spin reorientation transition (SRT) of epitaxial Co films in Au(111)/Co/X (X = UHV, W, Au). By means of magneto-optical Kerr effect, SQUID magnetometry, and polarized neutron reflectometry, we observe at 300 K the SRT at a Co thickness  $d^* = 9.6 \text{ \AA}$ ,  $12.8 \text{ \AA}$ , or  $14.5 \text{ \AA}$  for uncapped Co (X = UHV), and W or Au capping, respectively. The difference in  $d^*$  for W and Au capping strongly increases at lower temperatures, from  $1.7 \text{ \AA}$  at 300 K to  $10 \text{ \AA}$  at 10 K.

X-ray magnetic circular dichroism (XMCD) magnetometry provides evidence that the SRT also depends on the cap layer thickness. Whereas a  $20 \text{ \AA}$  Au capping exhibits a pure in-plane magnetization at 300 K, the same Co film with thinner capping shows a significant out-of-plane component. These findings are linked with the orbital moment of Co, which is evaluated from the XMCD data. We observe a 38% enhancement of the orbital moment per Co atom from 0.13 mB for  $20 \text{ \AA}$  Au cap to 0.18 mB for  $10 \text{ \AA}$  Au cap. Following the treatment by Bruno, the spin-orbit magnetic anisotropy energy of  $1.25 \times 10^{-4} \text{ eV}$  per Co atom is derived from the data. This energy is still larger than the spin-spin dipole interaction of about  $9 \times 10^{-5} \text{ eV}$  per Co atom. Hence, it explains qualitatively the observation of out-of-plane components as the Au cap thickness decreases.

### 4.4. Energy-dispersive detection of coherent x-ray scattering

U. Pietsch, T. Panzer, J. Grenzer, A. Pucher

University of Potsdam, Germany, Germany

E-mail: [upietsch@rz.uni-potsdam.de](mailto:upietsch@rz.uni-potsdam.de)

Coherent x-ray scattering is an attractive possibility for determining the phase correlation of a sample in space and time. X-ray correlation spectroscopy is usually performed at undulator beamlines of synchrotron radiation facilities in angular dispersive mode (fixed energy). We have applied the energy-dispersive mode for the first time. The experiment was performed at a bending-magnet beamline of BESSY II (Berlin). The white beam ( $5 < E < 20 \text{ keV}$ ) was guided through a  $0.005 \text{ mm}$  pin hole installed straight after the exit window of the beamline. Because of the coherence of synchrotron radiation, the diffracted beam provides "Fresnel rings" for a particular energy, which has to be selected by an energy-dispersive element. In our case, it was an energy-dispersive detector attached to a multichannel analyser. Although the energy resolution of the system is only about 1%, we found well selected Fresnel rings for energies between  $5 < E < 15 \text{ keV}$  recorded simultaneously at a distance of  $1.4 \text{ m}$  downstream by a detector scan and using a detector pinhole of  $0.010 \text{ mm}$ . Due to the relaxed energy-resolution, the intensity per step was on the order of  $1,000 \text{ cps}$ , which might be sufficient to perform time-correlation measurements in the time range of several tens of seconds to a few minutes. The experiment verifies that the x-ray energy-dispersive mode is suitable for the detection of coherent scattering phenomena.

#### 4.5. Porous silicon studies using x-ray grazing incidence techniques

V. Chamard,<sup>1</sup> G. Dolino,<sup>2</sup> P. Bastie,<sup>2</sup> D. Le Bolloc'h,<sup>3</sup> E. Elkaim,<sup>4</sup> C. Ferrero,<sup>3</sup> J.P. Lauriat,<sup>4</sup> F. Rieutord,<sup>5</sup> D. Thiaudiere,<sup>4</sup>

<sup>1</sup>Univ. Dortmund, Germany, <sup>2</sup>Laboratoire de Spectrometrie Physique, France, <sup>3</sup>ESRF, France, <sup>4</sup>LURE, France, <sup>5</sup>DRFMC/CEA, France

E-mail: [chamard@physik.uni-dortmund.de](mailto:chamard@physik.uni-dortmund.de)

Since the discovery of its visible luminescence at room temperature, porous silicon has raised a strong interest. However, the formation mechanisms are not completely understood. Information concerning the first steps of the formation can be obtained in a nondestructive way using x-ray grazing incidence techniques. Using Grazing Incidence Small Angle X-ray Scattering (GISAXS) at ESRF's ID1 beamline, we observed a systematic pore correlation for all porous silicon types. The quantitative analysis of the measurement was performed for the p-type sample using a simple spherical model of pores and an isotropic distribution of scattering particles. This led to a typical pore size of 6.2 nm and a particle-particle correlation length of 8.6 nm. In addition, for this type of porous silicon, the morphology of the surface and interface of the layer was studied by specular and off-specular reflectivity at LURE. The roughening due to the pore front propagation was quantified and the interface instability of p-type porous silicon was observed [1].

[1] V. Chamard et al., Phys. Rev. B 64 (2001) 245416.

#### 4.6. Structural and magnetic properties of EuSe/PbSe, EuSe/PbTe, and EuSe/EuTe superlattices grown by molecular beam epitaxy

R.T. Lechner,<sup>1</sup> T. Schüllli,<sup>1</sup> G. Springholz,<sup>1</sup> G. Bauer,<sup>1</sup> D. Lott,<sup>2</sup> A. Schreyer,<sup>2</sup> H. Clemens,<sup>2</sup> H. Krenn,<sup>3</sup>

<sup>1</sup>Johannes Kepler Universitaet Linz, Austria, <sup>2</sup>GKSS Forschungszentrum GmbH, Germany, <sup>3</sup>Karl Franzens Universität, Austria

E-mail: [dieter.lott@gkss.de](mailto:dieter.lott@gkss.de)

Magnetic multilayers (MLs) have attracted substantial interest because of the modifications of the magnetic interactions by strain, finite thickness, and interlayer couplings across magnetic or nonmagnetic spacer layers. The interest in these MLs is based on the heteroepitaxial growth of wide band gap Eu chalcogenide semiconductors EuX (X = O, S, Se, Te) on the lead salt layers by MBE since both groups of materials crystallize in the rock salt structure. The EuX compounds are classical Heisenberg magnets because of the exchange interactions between the localized magnetic moments of the half-filled 4f levels of Eu<sup>2+</sup> ions (spin 7/2). EuSe is particularly interesting because of its metamagnetic behaviour with a transition between different types of antiferromagnetic, ferrimagnetic as well as ferromagnetic structures as a function of temperature and magnetic fields. In the present work, a series of EuSe/PbSe, EuSe/PbTe and EuSe/EuTe MLs were grown by MBE on BaF<sub>2</sub> (111) substrates. Due to the differences in the lattices constants the biaxial strain state in the EuSe layers can be tuned over a large range from -6% to +1.6%. For structural characterisation anomalous diffraction measurements were performed. For the investigation of the magnetic properties SQUID magnetization as well as neutron diffraction (ILL) measurements were carried out. The first (ferro-), second (antiferro-) and third (ferrimagnetic) order Bragg peaks were investigated as functions of temperature and magnetic field to map phase diagrams. The results demonstrate a systematic influence of the strain state in the layers on the ferrimagnetic and antiferromagnetic phase transitions.

#### **4.7. The study of the structure and exchange coupling of the Py(Ni<sub>80</sub>Fe<sub>20</sub>)/Cr multilayers on sapphire substrates**

K.L. Yu,<sup>1</sup> M.Z. Lin,<sup>1</sup> C.H. Lee,<sup>1</sup> J.C.A. Huang,<sup>2</sup> Z.A. Ku,<sup>2</sup>

<sup>1</sup>National Tsing Hua University, Taiwan, <sup>2</sup>National Cheng Kung University, Taiwan

E-mail: [d867110@oz.nthu.edu.tw](mailto:d867110@oz.nthu.edu.tw)

The coupling between two permalloy layers with a Cr separating layer was studied using LMOKE, polarized neutrons, and XRD. The sample system in our study was Py(Ni<sub>80</sub>Fe<sub>20</sub>)/Cr multilayers epitaxied on different sapphire substrates with a Pt buffer layer. The crystal orientation was thought to be Al<sub>2</sub>O<sub>3</sub>//Pt(111)//Py(111)//Cr(110)//Py(111). From the LMOKE results, we found that the coupling between the two permalloy layers is AF when the Cr thickness is near 2.5 nm along the hard axis by a twofold symmetry. A preliminary neutron reflectivity study was done with the POSY1 reflectometer of IPNS at Argonne National Laboratory. From the results, it was determined that the coupling of the two moments of Py layers are collinear at the same direction at 200 Oe. The angle between the magnetic moment of each Py layer is less than 180 degrees at the lower applied field. When the applied field is near zero, the moment of Py layers is expected to be collinear along the easy axis in the opposite direction. To study the in-plane anisotropy of a sixfold symmetry system is still a puzzle. The anisotropy might be induced by some mechanisms such as strain-induced anisotropy from lattice mismatch of Py(111) on Cr(110), step-induced anisotropy, or interlayer biquadratic coupling. However, from the XRD result, it was determined that no significant strain variances of different in-plane directions can be observed. Because the Cr layer is too thin and disordered, the structure of the Cr layer is hard to know. Some miscut angle of the substrates was detected and seemed not to follow the hard-axis direction. Other AFM measurements were done, but no significant surface steps were observed. The possibility of step-induced anisotropy is slim.

#### **4.8. In situ neutron reflection study of the Li intercalation mechanism in thin film anatase TiO<sub>2</sub>**

M. Wagemaker, A.A. van Well, IRI TU Delft, Netherlands

E-mail: [m.wagemaker@iri.tudelft.nl](mailto:m.wagemaker@iri.tudelft.nl)

Neutron reflectometry is used to study the depth-dependent lithium density profile during intercalation. During lithium insertion, phase separation in a Li-rich and Li-poor region is established. The phase front is parallel to the surfaces and moves deeper into the electrode as more lithium is inserted. The major question was the mechanism of deintercalation because a difference in diffusion coefficient is found for insertion and extraction. The neutron reflection experiments prove that during deintercalation the phase front moves back to the surface, which is exactly the reverse of the intercalation. During electrochemistry, a thin, presumably organic, layer is formed, passivating the electrochemical performance.

#### 4.9. Quasi-in situ reflection mode EXAFS at the Ti/K edge of lithium intercalated rutile and mixed anatase/rutile TiO<sub>2</sub> thin films

M. Wagemaker,<sup>1</sup> D. Lützenkirchen-Hecht,<sup>2</sup> P. Keil,<sup>2</sup> R. Frahm,<sup>2</sup> A.A. van Well,<sup>1</sup>

<sup>1</sup>IRI TU Delft, Netherlands, <sup>2</sup>Bergische Universität Gesamthochschule Wuppertal, Germany

E-mail: [m.wagemaker@iri.tudelft.nl](mailto:m.wagemaker@iri.tudelft.nl)

The near-surface structure of Li-intercalated rutile and mixed anatase/rutile TiO<sub>2</sub> electrodes was investigated with grazing incidence reflection mode EXAFS spectroscopy. Although real in situ experiments are not feasible due to the extremely strong parasitic absorption of the electrolyte, a new cell was constructed that enables the electrochemical processing of samples sensitive to oxidation and permits reflection mode x-ray experiments after the controlled emersion of the electrodes from the electrolyte. During the electrochemical Li intercalation in pure rutile, only a thin surface layer of about 5 nm thickness was changed by the lithiation, whereas the mixed electrode was completely intercalated. Both intercalated layers seemed to have a structure similar to that of the Li-titanate Li<sub>0.5</sub>TiO<sub>2</sub> (anatase phase). The potential for Li-intercalation in rutile is significantly more cathodic compared to that of the anatase-containing electrode, which suggests that the more opened crystallographic structure of the anatase phase facilitates Li-intercalation into the lattice. The XANES and EXAFS regions change considerably upon lithiation, which can be explained in terms of changes in the electronic and crystallographic structure.

#### 4.10. Influence of x-ray illumination on thin Ti/C films

K.M. Zimmermann,<sup>1</sup> L. Bruegemann,<sup>1</sup> D. Weissbach,<sup>2</sup> R. Dietsch,<sup>2</sup> M. Tolan,<sup>3</sup>

<sup>1</sup>Bruker-AXS GmbH, Germany, <sup>2</sup>Fraunhofer IWS, Germany, <sup>3</sup>University Dortmund, Germany

E-mail: [martin.zimmermann@bruker-axs.de](mailto:martin.zimmermann@bruker-axs.de)

Thin Ti/C multilayers were deposited on silicon substrates using pulse-laser deposition [1]. X-ray reflectivity measurements up to 0.9 Å<sup>-1</sup> were performed in order to determine structural properties of those samples. A series of reflectivity measurements executed on the same sample showed stability of layer parameters. To study this behaviour in more detail, reflectivity measurements were executed in situ and ex situ on the sample under nonambient conditions. Traditional layered-structure model-based calculations did not lead to a satisfying agreement between measurement and simulation. The so-called inverse method applied on this investigation solved the analytical problem. The matching electron-density profiles (EPD) were obtained by analysing the height-height correlation function [2] and applying an inversion algorithm [3]. The measurements, the inversion algorithm, the resulting EPS's, and their unambiguousness will be discussed.

[1] R. Dietsch et al., Appl. Surf. Sci.: in press, 7993 (2002)

[2] C.-J. Yu et al, Phys. Rev. Lett.: 82, 2326 (1999)

[3] K. M. Zimmermann et al., Phys. Rev. B: 62, 10377 (2000)

#### 4.11. Deuterium in 001-oriented Mo<sub>0.5</sub>V<sub>0.5</sub>/V: the vanishing superlattice

V. Leiner,<sup>1</sup> H. Zabel,<sup>2</sup> J. Birch,<sup>3</sup> and B. Hjörvarsson<sup>4</sup>

<sup>1</sup>Institute Laue Langevin, France, <sup>2</sup>Ruhr-Universität Bochum, Germany, <sup>3</sup>Linköping University, Sweden, <sup>4</sup>Uppsala University, Sweden

E-mail: [leiner@ill.fr](mailto:leiner@ill.fr)

We have investigated the deuterium density profile in a Mo<sub>0.5</sub>V<sub>0.5</sub>/V superlattice along the direction parallel to the surface normal, using neutron reflectivity. The sensitivity to changes in the deuterium density profile at the interfaces was enhanced by careful selection of the thickness ratio of the constituents. Furthermore, the alloy composition of the Mo<sub>0.5</sub>V<sub>0.5</sub> layer was chosen so that no depletion zone of hydrogen (deuterium) is expected at the interface in the low concentration limit. The neutron reflectivity results yield, however, clear evidence of a depletion zone at the interfaces, with an extension of at least one monolayer. The appearance of a depletion layer is inferred to originate in the H–H interaction. Finally, by simultaneously monitoring the expansion and the concentration, we determined the elastic response of the V layers, and we proved the presence of nonlinear elastic response associated to a change-of-site occupancy.

#### 4.12. The ADAM reflectometer at ILL

V. Leiner,<sup>1</sup> H. Zabel,<sup>2</sup> M. Wolff,<sup>2</sup>

<sup>1</sup>Institute Laue Langevin, France, <sup>2</sup>Ruhr-Universität Bochum, Germany

E-mail: [leiner@ill.fr](mailto:leiner@ill.fr)

ADAM is a fixed-wavelength angle-dispersive reflectometer that combines strong performance and high flexibility. Operated at a wavelength of 0.441 nm, q-values up to 2 Å<sup>-1</sup> can be reached. We describe the instrument and the latest technical upgrades. To demonstrate the performance of the instrument, results from recent experiments are presented. The investigated systems include thin magnetic films, sheared liquids, neutron optical devices, and soft-matter systems.

#### 4.13. Resonant magnetic scattering of X rays from magnetically rough films in the DWBA

D.R. Lee<sup>1</sup> and S.K. Sinha<sup>2</sup>

<sup>1</sup>Argonne National Laboratory, USA, <sup>2</sup>University of California (San Diego), USA

E-mail: [drlee@aps.anl.gov](mailto:drlee@aps.anl.gov)

We present a formalism for treating the specular and diffuse resonant magnetic scattering of X rays from thin films and multilayers in which the interfaces possess both chemical and magnetic roughness and also magnetic domains. The calculations were done using the distorted wave Born approximation (DWBA). Numerical results are presented for single surfaces, thin films, and also for magnetic multilayers such as the Gd/Fe system.

Work at Argonne is supported by the U.S. Department of Energy under Contract No. W-31-109-ENG-38.

#### 4.14. Study of surface structural inhomogeneities of the MnO<sub>2</sub> thin films by small-angle x-ray scattering

L. Skatkov<sup>1</sup> and V. Gomofov,<sup>2</sup>

<sup>1</sup>PCB "Argo," 4/23 Shaul ha-Melekh Street, Israel<sup>2</sup>Kharkov Polytechnical University, Ukraine

E-mail: [lskatkov@surfnet.il](mailto:lskatkov@surfnet.il)

MnO<sub>2</sub> films that have been prepared by the thermal deposition of Mn(NO<sub>3</sub>)<sub>2</sub> are important semiconductor materials for application in thin film devices such as capacitor metal-dielectric semiconductor systems. For practical application of MnO<sub>2</sub>, the characteristics of surface structural inhomogeneities-submicropores (SMP) are critically important. In the present work the morphology, concentration, and size distribution of SMP in MnO<sub>2</sub> films were investigated by x-ray small-angle scattering (SAXS). We analyzed the following quantities: type of angular distribution; asymptotics and the integral parameters of the dispersion indices of SAXS related to the typical size  $l$ ; the typical volume  $V$ ; and the typical SMP shadow area  $f$ . Since the size distribution appeared to be polymodal, we classified the pores into four groups, according to their size  $R$ . The major contribution to the SMP volume concentration is made by SMP not exceeding 8 nm. The total share of SMP in MnO<sub>2</sub> films is about 9.8%, which agrees with the known value.

#### 4.15. Quantitative determination of the resonant magneto-optical constants at the Gd M<sub>4,5</sub> edges

J. Miguel,<sup>1</sup> J.F. Peters,<sup>1</sup> O.R.M. Toulemonde,<sup>1</sup> J.B. Goedkoop,<sup>1</sup> S. Dhesi,<sup>2</sup> N.B. Brookes,<sup>2</sup>

<sup>1</sup>University of Amsterdam, Netherlands, <sup>2</sup>ESRF, France

E-mail: [miguel@esrf.fr](mailto:miguel@esrf.fr)

Polarization-dependent soft x-ray resonant magnetic scattering is a new and promising technique for the study of nanomagnetic structures in surfaces and thin films. The resonant magnetic scattering cross section has three contributions. Quantitative knowledge of these three terms as a function of energy is important for the separation and quantification of the charge and magnetic contributions to the scattered intensity of complex nanomagnetic systems. We have determined the magneto-optical constants at the Gd M<sub>4,5</sub> edges by measuring the linear and circular absorption dichroism in transmission. The experimentally observed cross sections show an astounding quantitative agreement with atomic calculations obtained by using the Cowan code. The charge and circular dichroic and linear dichroic absorption cross sections form the imaginary part of the scattering cross section. The corresponding real parts can be obtained from these imaginary parts by Kramers–Kronig transformation. The total scattering cross sections thus obtained are compared with the energy-dependent scattered intensity from a magnetic stripe domain lattice. We show that the different energy dependencies allow the separation of the three different scattering contributions. It will be illustrated how this quantitative knowledge of the scattering cross sections can be used to unravel the structure of magnetic domain walls with a sensitivity of 5 nm.

#### 4.16. Spin-polarized neutron reflectivity and magnetization study of Nb/Al multilayers

S.W. Han,<sup>1</sup> J. Farmer,<sup>1</sup> P.F. Miceli,<sup>1</sup> G.P. Felcher,<sup>2</sup> R. Goyette,<sup>2</sup> G.T. Kiehne,<sup>3</sup> J.B. Ketterson,<sup>3</sup>

<sup>1</sup>University of Missouri-Columbia, USA, <sup>2</sup>Argonne National Laboratory, USA, <sup>3</sup>Northwestern University, USA

E-mail: [micelip@missouri.edu](mailto:micelip@missouri.edu)

We report the results of an initial investigation of superconducting Nb/Al multilayers where the magnetic field was applied parallel to the surface. Peaks are observed in the DC magnetization above the lower critical field ( $H_{c1}$ ), suggesting that there might be surface-induced vortex ordering in these systems. Spin-polarized neutron reflectivity (SPNR) was performed on a sample with 20 repeats of Nb(72 Å)/Al(20 Å), finding a London screening length of 1800 Å from low-field measurements. At higher fields, between 1500 and 2000 G, the reflectivity detects flux penetration with the flux lines located in the center of the film, to within 25% of the film thickness. A discussion will be presented on the ability to determine the flux line positions using the SPNR technique.

Funding support is acknowledged from the NSF DMR9623827, MISCON DOE DE-FGG02-90ER45427, as well as the University of Missouri Research Board. The Intense Pulsed Neutron Source at Argonne National Laboratory is funded by the U. S. Department of Energy, BES-Materials Sciences, under Contract No. W-31-109-Eng-38.

#### 4.17. Magnetism at a buried Co/Pd interface probed by standing-wave enhanced magnetic circular dichroism

S.K. Kim,\* J. Kortright, Lawrence Berkeley National Laboratory, USA

E-mail: [JBKortright@lbl.gov](mailto:JBKortright@lbl.gov)

Magnetism in ultrathin films exhibits a wide range of behaviors, including enhanced and suppressed moments and magnetic reorientation transitions. Co ultrathin layers between Pt or Pd show both enhanced orbital and spin moments and reorientation to perpendicular magnetization when the Co thickness  $t_{Co} < 1$  nm. We probed Co interfacial magnetism when  $t_{Co} = 2$  nm and the layer retains in-plane anisotropy to look for precursor effects of the magnetic reorientation transition. The Pd/Co/Pd trilayer was deposited directly atop a W/B<sub>4</sub>C multilayer interference structure designed to generate an x-ray standing wave (SW) that could be scanned through a Co/Pd interface [1]. Co  $L_{2,3}$  absorption and MCD spectra were measured revealing the variation of the number of Co  $d$  holes  $n_d$  and effective spin  $m_s$  and orbital  $m_l$  moments as the SW position was varied across the Co on Pd interface into the center of the Co layer. A large interfacial enhancement in  $n_d$  was observed, consistent with charge transfer from Co to Pd at the interface. A modest enhancement in  $m_s$  and a large enhancement in  $m_l$  were also observed at the interface. Because these moments were measured predominantly along the in-plane direction, the enhanced Co interfacial  $m_l$  developed first with an in-plane orientation, before  $m_s$  and  $m_l$  reoriented to perpendicular as  $t_{Co}$  was reduced. This behavior reveals that the common two-term anisotropy model of the transition from in-plane to perpendicular anisotropy is oversimplified, since the interface term is not constant with  $t_{Co}$  during this transition.

This work was supported by the U.S. Department of Energy under Contract No. DE-AC03-76SF00098.

\*Current address, Seoul National University, Seoul, South Korea.

[1] Sang-Koog Kim and J. B. Kortright, Phys. Rev. Lett. 86, 1347 (2001).

#### **4.18. Structure determination of submonatomic Sn layers in Fe/Cr(Sn)Cr magnetic multilayers using anomalous x-ray scattering techniques**

K. Ishiji, H. Okuda, N. Hosoi, H. Hashizume, Nara Inst. of Sci. and Tech, Japan  
E-mail: [hhashizu@ms.aist-nara.ac.jp](mailto:hhashizu@ms.aist-nara.ac.jp)

The structures of [Fe/Cr(Sn)Cr]<sub>39</sub> superlattices with submonatomic Sn layers embedded in the Cr layers have been determined by x-ray reflectivity and diffuse scattering measurements. The scattering contrast between the nanometer-thick Fe and Cr layers was controlled using the anomalous dispersion technique at synchrotron sources. In the samples investigated, the submonatomic Sn is likely to form ultrathin layers from 0.05 to 0.2 nm in thickness within the Cr layers. The Cr/Sn interfaces have a roughness structure similar in mean-square roughness and in-plane cutoff length to the Fe/Cr interfaces. The roughness structures of both Cr/Sn and Fe/Cr interfaces are highly correlated through the entire superlattice. This work demonstrates the power of the x-ray scattering near the absorption edges in the study of the structure of ultrathin Sn layers less than a monolayer thickness.

#### **4.19. Structural characterization of ZnO/Al<sub>2</sub>O<sub>3</sub>(11-20) and Au/ZnO/Al<sub>2</sub>O<sub>3</sub>(11-20) films by x-ray scattering**

M. Ay, A. Nefedov, H. Zabel, Ruhr-Universität Bochum, Germany  
E-mail: [murat.ay@ruhr-uni-bochum.de](mailto:murat.ay@ruhr-uni-bochum.de)

We studied the possibility of growing O-terminated ZnO(000-1) films on Al<sub>2</sub>O<sub>3</sub> substrates with high structural quality. After growth via sputtering methods, the ZnO films were annealed to increase the film quality, resulting in a mosaicity of 0.66° and a surface roughness of less than 3 Å. Finally, gold films were sputtered at different temperatures on this ZnO(000-1) surface. The structural properties of the samples were investigated by x-ray scattering methods, reflection high-energy electron diffraction (RHEED), and atomic force microscopy (AFM). X-ray measurements were performed at the W1 beamline at the HASYLAB in Hamburg and with a rotating anode generator in Bochum ( $\lambda = 1.542 \text{ \AA}$ ). X-ray diffraction shows the [111] out-of-plane texture of Au. Measurements at grazing incidence show the in-plane single domain growth of ZnO(000-1) on Al<sub>2</sub>O<sub>3</sub> (11-20) and also of Au(111) on ZnO(000-1). The azimuthal orientations Au[1-10] || ZnO[11-20] and Au[11-2] || ZnO[10-10] lead to a lattice mismatch of -11.4%. The epitaxial relation between the ZnO and Au atoms is due to a 8:9 supercell commensuration, with a lattice mismatch of 0.58%. AFM images clearly demonstrate that gold films form clusters in a defined temperature range.

#### **4.20. Improved compact x-ray sources**

A. Mozelev, RADICAL, Austria

E-mail: [mozelev@technologist.com](mailto:mozelev@technologist.com)

The main focus of this research is examination of the source of artificial x-ray radiation. The up-to-date methods of researching radiation effects are usually based on the spectrometry of scattering irradiations excited by different radioisotopic sources. Preliminary computation and mathematical simulation have revealed that the x-ray generator has advantages over the traditional radioisotope sources in technical characteristics. The remote handling of physical parameters (intensity, energy of gamma quants, etc.) makes it possible to use a gamma quant generator in different areas of science and technique. The designing of the generator was intended for the most difficult application case—a deep borehole with high temperatures and high pressure. It was necessary to minimize dimensions and the power the generator needed, and this has resulted in the minimum possible impulse duration. Several variants of vacuum tubes were researched; the results are cited. If we have diameter of the vacuum tube  $D = 90$  mm, the kinetic energy of electron  $E = 1$  MeV;  $D = 70$  mm,  $E = 700$  KeV;  $D = 60$  mm,  $E = 500$  KeV ;  $D = 45$  mm,  $E = 150$  KeV. In the course of investigation, a model generator was created. Carrying out research with this model has also shown the expediency of subsequent investigations to confirm theoretical computations. As a result of the research, the following parameters have been received: diameter less than 70 mm; length less than 300 mm; weight less than 2 kg. Electron source specification: kinetic energy 500 KeV; pulse duration 10 ns; impulse frequency 0.5–50 Hz.

\* \* \*

**SESSION NO. 5, 8:30 AM**  
**WEDNESDAY, 25 SEPTEMBER 2002**  
**FILM GROWTH AND SURFACE STRUCTURE — II**  
**GRANLIBAKKEN CONFERENCE CENTER LAKE-BAY ROOM**

**5.1. Use of coherent x-ray diffraction to image surface structure (Invited)**

I.K. Robinson, Univ. of Illinois at Urbana-Champaign, USA

E-mail: [robinson@mrl.uiuc.edu](mailto:robinson@mrl.uiuc.edu)

New possibilities for structure determination with x rays have appeared with the development of third-generation sources of synchrotron radiation. In this talk, I will discuss my progress towards achieving this goal. The reflection of a coherent x-ray beam from a rough surface contains fine diffraction features that are the Fourier transform of a phase object representing the morphology. Because the diffraction is continuous, it can be oversampled and thus inverted to an image. I will demonstrate this with experiments on the real-time oxidation of silicon wafers. I will also discuss a second application to the inversion of crystal truncation rods from layered structures, which relates to crystallographic "direct methods."

**5.2. X-ray scattering measurements of concentration enhanced interdiffusion at Si/SiGe interfaces**

D.B. Aubertine, N. Ozguven, A.F. Marshall, P.C. McIntyre, Stanford University, USA

E-mail: [auber@stanford.edu](mailto:auber@stanford.edu)

The thermal stability of Si/SiGe interfaces may be limited by an enhanced Si-Ge interdiffusivity that is often observed during the early stages of annealing. In an effort to characterize this effect, interdiffusion and strain relaxation at Si/SiGe interfaces are simultaneously measured via synchrotron-source x-ray diffraction from Si/SiGe superlattices. Both symmetric and asymmetric diffraction geometries and transmission electron microscopy analysis of misfit dislocation structures have been used to characterize the dynamics of misfit strain relief during post-deposition annealing of CVD-grown epitaxial multilayers. Interdiffusion kinetics were determined by measurement of the attenuation of superlattice x-ray satellite peaks after high-temperature annealing. Based on this work, we show that the enhanced interdiffusion can be accurately modeled by accounting for the concentration dependence of the activation enthalpy and exponential prefactor for Si/SiGe interdiffusion. We further demonstrate that, by comparison, strain enhancement of Si/SiGe interdiffusion is a secondary effect.

### 5.3. Grazing incidence small angle x-ray scattering for measuring particle/pore-size distributions in thin films

K. Omote, Y. Ito, K. Inaba, Rigaku Corporation, Japan  
E-mail: [omote@rigaku.co.jp](mailto:omote@rigaku.co.jp)

A grazing incidence small-angle x-ray scattering technique has been developed for characterizing nano-particle/pore structure in thin films. Small angle scattering data are measured by using offset  $2\theta-(\theta + \delta)$  scans and  $(\theta\text{-fixed})-2\theta$  scans, in order to avoid strong specular reflections from the film surface and its substrate. We have calculated scattering cross sections of X rays by the particle/pore structures, taking into account reflection and refraction at the surface and interfaces based on distorted wave Born approximation (DWBA). For the quantitative analysis of particle/pore-size distribution in the film, a gamma-distribution model is employed in the calculation. We also have considered the contribution of surface diffuse scattering calculated by the DWBA. The  $(\theta\text{-fixed})-2\theta$  scans are used for estimating the contribution from the surface diffuse scattering. The average diameter, variance of the gamma-distribution function, and parameters of the surface morphology are varied and refined by computer so that the calculated scattering pattern best matches the experimental pattern. The technique has been applied to analyze pore-size distribution in porous low-k films, which are extensively studied for lowering the dielectric constant of an interlayer insulator. Such low dielectric constant materials are required to reduce RC delay of Cu intermediate wiring, which will be less than 10 nm in the near future. The pore size distributions determined by the present small angle x-ray scattering technique agree with that of the commonly used gas adsorption technique. We will also present a particle-size distribution in nanogranular thin films.

### 5.4. Vertical alignment of GaN quantum dots stacked in multilayers: correlation-length, depth-resolved strain analysis and elastic energy distribution

V. Chamard,<sup>1</sup> T.H. Metzger,<sup>2</sup> V. Holý,<sup>3</sup> M. Sztucki,<sup>2</sup> M. Tolan,<sup>1</sup> E. Bellet-Amalric,<sup>4</sup> B. Daudin,<sup>4</sup> C. Adelmann,<sup>4</sup> H. Mariette,<sup>4</sup>  
<sup>1</sup>Univ. Dortmund, Germany, <sup>2</sup>ESRF, France, <sup>3</sup>Laboratory of Thin Films and Nanostructures, Masaryk University, Czech Republic, <sup>4</sup>CEA-CNRS joint group, France  
E-mail: [chamard@physik.uni-dortmund.de](mailto:chamard@physik.uni-dortmund.de)

The current interest in self-organized growth of strained semiconductor nanostructures is based on the possibility of achieving novel optical and electronic properties. Among them, nitride compounds are especially interesting due to their application in the blue-UV wavelength range. Using the Stranski–Krastanow growth mode, GaN dislocation-free quantum dots (QDs) are obtained [1]. For application, the QDs are embedded in an AlN matrix and stacked in multilayers. The dots are believed to be vertically aligned along the threading dislocation edges. The resulting structure is investigated by x-ray grazing incidence techniques, which are nondestructive and provide depth resolution, averaged over a large number of QDs [2]. Applying grazing incidence small angle scattering, we have quantified the strong vertical alignment of the dots and observed its dependence with the spacer layer thickness and repeat unit number, showing a strain-induced mechanism for the dot vertical ordering. The strain analysis was performed using chemically sensitive anomalous grazing incidence diffraction, near to and far from the absorption edge of the Ga: the strain states of the dots and of the multilayer surrounding matrix were identified. Finally, elastic energy distribution induced by a GaN buried dot and calculated for different AlN spacer layer thicknesses explained the origin of the vertical alignment. Both experimental and calculation results are compared with other systems (GaAs/InAs).

[1] B. Daudin, et al., Phys. Rev. B 56, R7069 (1997).

[2] V. Chamard, et al., Appl. Phys. Lett. 79, 1971 (2001).

## 5.5. Determination of absolute indium content in InGaN/GaN multiple quantum wells using anomalous x-ray scattering

D.Y. Noh,<sup>1</sup> H.H. Lee,<sup>1</sup> K.S. Liang,<sup>2</sup>

<sup>1</sup>K-JIST, South Korea, <sup>2</sup>SRRC, Taiwan

E-mail: [dynoh@kjist.ac.kr](mailto:dynoh@kjist.ac.kr)

We have determined the absolute indium content incorporated in the crystalline lattice of InGaN films and InGaN/GaN multiple quantum wells using anomalous x-ray scattering (AXS). AXS spectra were obtained near the In *K* absorption edge at the InGaN (0006) Bragg peak where the InGaN Bragg reflection is well resolved from the GaN reflections. By comparing the indium composition obtained by AXS to regular x-ray scattering results, which are also sensitive to the lattice strain, we determined the Poisson's ratio of InGaN,  $n \approx 0.23$ . The AXS method can be an effective method of determining the absolute chemical composition of InGaN independent of the lattice strain, which is especially valuable for the InGaN multiple quantum wells.

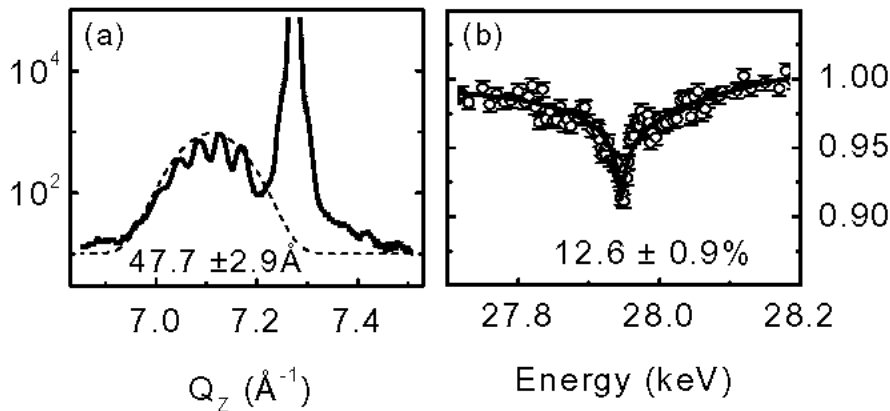


**Figure 1** (a) Diffraction profile of the (0006) InGaN/GaN multiquantum well. (b) AXS obtained near the In *K* absorption edge.

\* \* \*

**SESSION No. 6, 11:00 AM**  
**WEDNESDAY, 25 SEPTEMBER 2002**  
**SOFT X RAYS**  
**GRANLIBAKKEN CONFERENCE CENTER LAKE-BAY ROOM**

**6.1. Magnetic x-ray scattering as a probe of heterogeneous magnetic thin films (Invited)**

E.E. Fullerton, IBM Almaden Research Center, USA  
E-mail: [eef@almaden.ibm.com](mailto:eef@almaden.ibm.com)

The element-specificity of resonant magneto-optical effects near core levels in the x-ray range offers numerous opportunities to study the magnetism in high-coercivity thin films. Resonant small-angle scattering (SAS) is a particularly powerful technique for exploring the magnetic properties of heterogeneous films. At the 1–2 nm wavelengths of interest, SAS is readily measured from lateral inhomogeneities with dimensions comparable to or greater than these wavelengths and provides a quantitative measure of statistically averaged parameters such as average grain size and grain-size distributions. By tuning near resonances of selected elements, the scattering contrast can be enhanced and element-specific information (both structural and magnetic) determined. This approach is applied to explore the interplay of structural heterogeneities and magnetic domain structure in films of interest, such as advanced magnetic recording media. Recent examples of measurements at the Advanced Light Source at Lawrence Berkeley National Laboratory on CoPtCr alloy films, Co/Pt multilayers, and chemically synthesized self-organized particles will be discussed. Comparisons with magnetic imaging and the potential use of a coherent source (i.e., speckle) will be highlighted.

This work was done in collaboration with Olav Hellwig, Jeff Kortright, Greg Denbeau, Steve Kevan, Michael Pierce, Rob Moore, Phillip Geissbuhler, and Larry Sorensen.

**6.2. Resonant small-angle x-ray scattering of polymers at the Carbon K edge**

I. Koprinarov,<sup>1</sup> G. Mitchell,<sup>2</sup> B. Landes,<sup>2</sup> J. Lyons,<sup>2</sup> B. Kern,<sup>2</sup> M. Devon,<sup>2</sup> J.B. Kortright,<sup>3</sup>  
<sup>1</sup>McMaster University, Canada, <sup>2</sup>The Dow Chemical Company, USA, <sup>3</sup>Lawrence Berkeley National Laboratory, USA  
E-mail: [IKoprinarov@lbl.gov](mailto:IKoprinarov@lbl.gov)

We are exploring the use of resonant x-ray scattering at the C1s ionization edge to enhance small-angle x-ray scattering of polymers. Resonant x-ray scattering is a well-known phenomenon and has been demonstrated for hard x-ray energies, but to our knowledge it has never before been attempted at the C1s edge. We have performed proof of principle experiments using mixtures of latex made from different polymers and dried onto x-ray transparent windows, and also using a thin film of one polymer phase dispersed into a matrix of another polymer. In the latter case, neither hard x-ray scattering nor electron microscopy had useful contrast because the matrix and dispersed phases were similar in density. Here the resonant C edge scattering provides key information unavailable by any other means. In the latex samples, strong resonant scattering enhancements are seen at the C edge, and the spectral shape of these enhancements depends sensitively on the specific polymer constituting the latex. In the case of the phase-separated polymers, the spectral difference in resonant enhancements of the different phases enhances scattering contrast and makes the analysis possible. The early results are very exciting and indicate that this technique may have several interesting and useful applications in the field of polymer characterization.

J. Kortright and work at Lawrence Berkeley National Laboratory were supported by the U.S. Department of Energy under Contract No. AC03-76SF00098.

### **6.3. Detailed study of magnetic reversal in stripe domain systems using resonant x-ray magnetic scattering**

J.F. Peters,<sup>1</sup> J. Miguel,<sup>1</sup> O.R.M. Toulemonde,<sup>1</sup> J.B. Goedkoop,<sup>1</sup> S. Dhesi,<sup>2</sup> N.B. Brookes,<sup>2</sup>

<sup>1</sup>University of Amsterdam, Netherlands, <sup>2</sup>ESRF, France

E-mail: [jfpeters@science.uva.nl](mailto:jfpeters@science.uva.nl)

We show how polarization-dependent resonant soft x-ray magnetic scattering can be used to separate the vector components of complicated magnetic stripe domain structures. By fitting the scattering data to micromagnetic models, we are able to reconstruct the 3D structure with a sensitivity up to 5 nm. This method is used to follow the evolution of the stripe system over the in-plane magnetization curve. We find that the evolution of the stripe structure over the magnetization curve shows an unexpected and amazingly rich behaviour, involving an disorder-order transition at the nucleation field, a strong dependence of the period on field, the creation and growth of a Bloch wall structure, and the appearance of closure domains. Between remanence and the coercive field, the Bloch wall structure is found to evolve into a Néel wall-type structure, which at remanence jumps back into a Bloch wall structure with the opposite magnetization direction. Interestingly enough, no trace of this discontinuous domain wall reversal is found back in the stripe period.

### **6.4. Probing thin film magnetic domain structures by resonant soft x-ray small angle scattering**

O. Hellwig,<sup>1</sup> J.B. Kortright,<sup>2</sup> E.E. Fullerton,<sup>1</sup>

<sup>1</sup>IBM Almaden Research Center, USA, <sup>2</sup>Lawrence Berkeley National Laboratory, USA

E-mail: [olav@us.ibm.com](mailto:olav@us.ibm.com)

We have exploited synchrotron radiation in the soft x-ray range to characterize the magnetic reversal behavior and domain structure in a variety of thin film systems. The magnetic films have been deposited onto SiN membranes in order to perform small angle scattering (SAS) experiments in transmission geometry. Controlling both, the energy and polarization of the X rays allows us to extract detailed information about the magnetic microstructure of the samples. Thus, we can probe the scattering intensity depending on the momentum transfer  $q$  or applied field  $H$  for a given energy and polarization. The experimental setup allows us to apply magnetic fields of up to 15 kOe and temperatures of between 20 and 300 K. As a result, it is possible to study the magnetic microstructure of a macroscopic area over a wide parameter range.

In this contribution, we will present different examples to highlight the great future potential of soft x-ray SAS techniques for the characterization of magnetic thin film systems. These examples include exchange bias systems and antiferromagnetically coupled layers to demonstrate the wide applicability of soft X rays in magnetism. Measurements were performed at beamlines 4, 6, and 8 at the Advanced Light Source, Berkeley, CA.

Work at Lawrence Berkeley National Laboratory was supported by the Director, Office of Energy Research, Office of Basic Energy Sciences, MSD, of the U.S. Department of Energy under Contract No. DE-AC03-76SF00098. O. Hellwig was supported by the Deutsche Forschungsgemeinschaft via a Forschungsstipendium under Contract Number HE 3286/2-1.

## 6.5. Magnetic x-ray reflectivity study of an Fe/Cr multilayer

D. Lott,<sup>1</sup> C.C. Kao,<sup>2</sup> C. Sanchez-Hanke,<sup>2</sup> G.P. Felcher,<sup>3</sup> J.S. Jiang,<sup>3</sup> S.D. Bader,<sup>3</sup>

<sup>1</sup>GKSS Forschungszentrum GmbH, Germany, <sup>2</sup>Brookhaven National Laboratory, USA, <sup>3</sup>Argonne National Laboratory, USA

E-mail: [dieter.lott@gkss.de](mailto:dieter.lott@gkss.de)

Determining the magnetic structure and magnetization profiles of thin magnetic layers and multilayers has become an important issue among material scientists and device designers. In this work, we report measurements of the charge and magnetic x-ray reflectivity of an Fe/Cr double-multilayer. The sample consists of a ferromagnetic [FM] Fe/Cr multilayer of five periods [Fe 50 Å/Cr 20 Å] on top of an antiferromagnetic [AF] Fe/Cr multilayer of 20 periods [Fe 14.5 Å/Cr 11.5 Å] and shows an “exchange bias” behavior after the AF is aligned with large external fields [1]. The focus of this work is on the magnetic structure of the multilayers. The experiments were carried out at the NSLS and APS using an elliptically polarized wiggler or diamond phase retarder to produce circularly polarized X rays. The element specificity of the method of magnetic x-ray reflectivity allows the separate investigation of the magnetic moments of Fe or Cr. The magnetic reflectivity curves clearly show features corresponding to the FM and AF contributions of both the Fe and Cr layers. Charge and magnetic reflectivity data were modeled using simulations based on the magneto-optical approach to determine the direction of the magnetic moments, the thickness of the magnetic layers, as well as the size of the optical magnetic constant. Determination of the magnetization profile of the system gives further insight into the magnetic coupling between the Fe and Cr layers.

[1] J.S Jiang, G.P Felcher, A. Inomata, R. Goyette, C.S Nelson, and S.D Bader, Phys. Rev. B 61, 9653 (2000).

\* \* \*

**SESSION NO. 7, 7:30 PM**  
**WEDNESDAY, 25 SEPTEMBER 2002**  
**SCATTERING FROM SOFT MATTER & LIQUIDS**  
**GRANLIBAKKEN CONFERENCE CENTER PAVILION**

**7.1. Interaction of the antimicrobial frog peptide, PGLa, with lipid monolayers studied by x-ray grazing incidence diffraction and reflectivity**

O. Konovalov,<sup>1</sup> K. Lohner,<sup>2</sup> I. Myagkov,<sup>3</sup> B. Struth,<sup>1</sup>

<sup>1</sup>European Synchrotron Radiation Facility, France, <sup>2</sup>Institute für Biophysik und Röntgen-  
strukturforschung, Austria, <sup>3</sup>Research Institute for Physical Problems, Russia

E-mail: [konovalo@esrf.fr](mailto:konovalo@esrf.fr)

We present a first study using synchrotron grazing incidence diffraction (GID) and x-ray reflectivity (XRR) measurements on mixed phospholipid/peptide monolayers at the air/water interface. Surface pressure/potential-area isotherms showed that the antimicrobial frog skin peptide, PGLa, formed a very stable monolayer with 2 PGLa molecules per kinetic unit and a collapse pressure of ~22 mN/m. X-ray GID indicated that the peptide-dimer formation did not lead to self-aggregation with subsequent crystallite formation. However, the scattering length density profile derived from XRR measurements yields information on the PGLa monolayer that protrudes into the air phase by about 8 Å, suggesting that the peptide is aligned parallel to the water surface. The monolayers composed of disaturated phosphatidylcholines and phosphatidylglycerols were stable up to 60 mN/m and exhibited a first-order transition from a liquid-expanded to a liquid-condensed state around 10 mN/m. Structural details of the phospholipid monolayers in the presence and absence of PGLa were obtained from synchrotron experiments. Thereby, the x-ray data of distearoylphosphatidylcholine/PGLa can be analyzed by the composition of its individual components, while the peptide strongly perturbs the lipid acyl chain order of distearoylphosphatidylglycerol. These results are in agreement that PGLa mixes at a molecular level with negatively charged lipids but forms separate islands in zwitterionic phosphatidylcholine monolayers, and demonstrate that antimicrobial peptides can discriminate between the major phospholipid components of bacterial and mammalian cytoplasmic membranes.

**7.2. Growth control of organic thin films**

B. Nickel,<sup>1</sup> L. Casalis,<sup>1</sup> M.F. Danisman,<sup>1</sup> G. Scoles,<sup>1</sup> S. Ianotta,<sup>2</sup> R. Ruiz,<sup>3</sup>

<sup>1</sup>Princeton Univ., USA, <sup>2</sup>Instituto di Fotonica e Nanotechnologie CNR, Italy, <sup>3</sup>Vanderbilt Univ., USA

E-mail: [nickel@princeton.edu](mailto:nickel@princeton.edu)

We have studied the thin-film formation of pentacene on metallic and inert surfaces with an emphasis on growth control. We demonstrate that chemical surface treatment allows one to tune the growth pattern in a broad range. Furthermore, we demonstrate that a new approach that involves a nonthermal increase of the deposition energy of the impinging molecules allows for the growth of thin films in cases where thermal evaporation fails. Our study is based on x-ray reflectivity, x-ray truncation rod interference measurements, rocking scans line shape analysis, and complementary He-atom diffraction data. In some cases, we compare our results to AFM data.

### 7.3. Neutron reflection from the liquid/liquid interface

J. Webster,<sup>1</sup> A. Zarbakhsh,<sup>2</sup> J. Bowers,<sup>3</sup>

<sup>1</sup>ISIS, United Kingdom, <sup>2</sup>Queen Mary, United Kingdom, <sup>3</sup>Exeter University, United Kingdom

E-mail: [j.r.p.webster@rl.ac.uk](mailto:j.r.p.webster@rl.ac.uk)

Neutron reflectivity has been used successfully to probe the oil/water interface, For the first time, structural determinations have been made using a nonvolatile oil phase.

### 7.4. Model lung surfactant lipid monolayers and the influence of pulmonary surfactant B on the lipid phase behaviour

F. Bringezu,<sup>1</sup> G. Brezesinski,<sup>2</sup> J.A. Zasadzinski,<sup>3</sup> J. Ding,<sup>3</sup> A. Waring,<sup>4</sup>

<sup>1</sup>University of Leipzig, Germany, <sup>2</sup>Max Planck Institute of Colloids and Interfaces, Germany, <sup>3</sup>University of California Santa Barbara, USA, <sup>4</sup>UCLA, USA

E-mail: [brif@medizin.uni-leipzig.de](mailto:brif@medizin.uni-leipzig.de)

Lung surfactant is a mixture of lipids and proteins forming a monolayer at the liquid/air interface in the lung alveoli. Key components mimicking many of the features of native surfactants both in vitro and in vivo are dipalmitoylphosphatidylcholine (DPPC), phosphatidylglycerols (PG), and palmitic acid (PA) as lipid components and the lung surfactant apoproteins B and C. In this study, grazing incidence x-ray diffraction measurements (GIXD), pressure-area isotherms and Brewster angle microscopy show that palmitic acid induces changes in the physicochemical parameters and molecular organization of lung surfactant lipid monolayers. GIXD indicates that PA interacts specifically with DPPC to form a mixed crystalline solid phase. Increasing PA content is roughly equivalent to increasing the surface pressure or decreasing the temperature of DPPC/POPG monolayers. The SP-B lipid interaction on the lipid phase behavior of a model mixture of DPPC/POPG/PA shows that SP-B alters the physicochemical parameters and structures of the lipid chain lattice. In the comparison of the full-length SP-B<sub>1-78</sub> with the shorter dimeric sequence dSP-B<sub>1-25</sub>, the latter shows the larger effects, suggesting the essential role of the dimeric structure for the peptide function. This presentation gives an insight into the function of the protein, which could help in engineering of lung surfactant replacements that are urgently needed in RDS therapy.

### 7.5. X-ray scattering studies on InGaAs quantum dots

C.-H. Hsu,<sup>1</sup> Y.P. Stetsko,<sup>1</sup> H.Y. Lee,<sup>1</sup> N.T. Yeh,<sup>2</sup> J.-I. Chyi,<sup>2</sup> D.Y. Noh,<sup>3</sup> M.T. Tang,<sup>1</sup> K.S. Liang,<sup>1</sup>

<sup>1</sup>SRRC, Taiwan, <sup>2</sup>National Central University, Taiwan, <sup>3</sup>Kwangju Institute of Science and Technology, South Korea

E-mail: [chsu@srcc.gov.tw](mailto:chsu@srcc.gov.tw)

We present a structural investigation of self-assembled InGaAs quantum dots on GaAs(001) substrates grown by molecular-beam epitaxy. The grazing incidence x-ray scattering measurements were performed at both BL17B of the Taiwan Light Source and BL12B2 of SPring-8. Scattering intensity profiles, both around Bragg points and at small angles, were collected. Model calculations of the x-ray intensity distribution curves were performed for data analysis. The strain field, composition distribution, and shape of the dots so obtained will be presented.

## 7.6. Investigation of confined and thin film polymers using x-ray scattering methods

O.H. Seeck,<sup>1</sup> M. Mihaylova,<sup>1</sup> H. Kim,<sup>2</sup> S.K. Sinha,<sup>2</sup> D. Lambreva,<sup>3</sup> Y. Serero,<sup>3</sup> W. deJeu,<sup>3</sup>

<sup>1</sup>FZ Juelich GmbH, Germany, <sup>2</sup>University of California (San Diego), USA, <sup>3</sup>AMOLF, Netherlands

E-mail: [ohseeck@mail.desy.de](mailto:ohseeck@mail.desy.de)

The properties of thin film polymers such as density profiles, surface parameters and molecular ordering close to hard walls, polymer/polymer junctions, and free polymer surfaces are the subject of the presented investigations. The studies have been carried out using x-ray reflectivity and diffuse scattering methods, depending on the molecular weight, the temperature, film thicknesses, and preparation of the substrate material. Grazing incidence diffraction methods have also been tried. Rather complete pictures of the thin film polymer properties could be gained in this way.

## 7.7. X-ray scattering at metal/polymer interfaces

R. Weber,<sup>1</sup> I. Grotkopp,<sup>1</sup> V. Chamard,<sup>2</sup> J. Stettner,<sup>1</sup> W. Press,<sup>3</sup> M. Tolan,<sup>2</sup> O.H. Seeck,<sup>4</sup>

<sup>1</sup>Institut fuer Experimentelle und Angewandte Physik, Germany, <sup>2</sup>Univ. Dortmund, Germany, <sup>3</sup>Institut Laue-Langevin, France, <sup>4</sup>FZ Juelich GmbH, Germany

E-mail: [chamard@physik.uni-dortmund.de](mailto:chamard@physik.uni-dortmund.de)

Polymer-protected, nanosized noble metals are receiving increased attention since they have many technological applications. For instance, depending on the structural properties of the gold colloids, a large luminescence range in the visible spectrum can be obtained. Moreover, polymer films containing metal clusters have been successfully tested as very active and selective catalytic membranes [1]. In order to control the properties of these systems, an accurate knowledge of the cluster structure and of the metal/polymer interface is needed. In some systems, a self-organization of the clusters is observed [2]. The origin of this process is still not clear.

Vacuum deposition of gold on polymer surfaces can lead to the formation of a layer of clusters with radii ranging from one to a few nanometers. When heated up to temperatures above the polymer glass transition, an embedding process occurs, which is driven by the decrease of the surface energy. Since this process only starts at a sufficiently low viscosity, the clusters may be used in order to monitor the onset of the glass transition of the polymer in the surface region. It will be shown that x-ray reflectivity (HASYLAB, DESY) is a very sensitive probe to study this onset via measuring the laterally averaged electron density profile for 100 nm thick polystyrene films [3]. The in-plane motion/growth of the clusters is studied with grazing incidence small angle x-ray scattering (GISAXS at ID1 beamline, ESRF).

[1] Clusters and Colloids: From Theory to Applications, edited by G. Schmid (VCH, Weinheim, 1994).

[2] A. Mayer and M. Anonietti; Colloid Polym Sci. 276, 769 (1998).

[3] R. Weber et al., Phys. Rev. E. 64, 61508 (2001).

## 7.8. Generic phase behavior of branched-chain phospholipid monolayers

G. Brezesinski,<sup>1</sup> F. Bringezu,<sup>2</sup>

<sup>1</sup>Max Planck Institute of Colloids and Interfaces, Germany, <sup>2</sup>University of Leipzig, Germany

E-mail: [brezesinski@mpikg-golm.mpg.de](mailto:brezesinski@mpikg-golm.mpg.de)

Monolayers of chemically modified triple-chain phospholipids have been investigated at the air/water interface using pressure-area isotherms. The condensed phases of the lipids were characterized by grazing incidence x-ray diffraction (GIXD). Increasing chain length corresponds to a temperature effect, which was quantified for different lipids, depending on the head group structure, using isotherm (2D systems) and DSC (3D systems) measurements. The combination with structure investigations revealed generic phase diagrams describing the phase behavior of multiple-chain lipids in two dimensions. For the 1-acyl-2-O-alkyl phospholipids, the generic phase diagram exhibits only  $L_{2d}$ , LS, and LE phases, while exchanging the position of the branched acyl and the nonbranched alkyl chains at the glycerol backbone leads to a much richer polymorphism ( $L_{2h}$ ,  $L_{2d}$ , Ov, LS, S,  $\tau$ , LE). Here we present the first experimental evidence of the unusual  $\tau$ -phase, which exhibits an undistorted in-plane lattice despite tilted chains in the case of multiple-chain lipid monolayers.

## 7.9. Neutron reflectivity applied to DNA chips

F. Cousin, A. Menelle, F. Boué, Laboratoire Léon Brillouin, France

E-mail: [cousin@llb.saclay.cea.fr](mailto:cousin@llb.saclay.cea.fr)

DNA chips are 2D biosensors able to detect simultaneously a large number of genes in a given solution. The detection of a specific gene is realized on each pixel of the chip: a complementary DNA strand to the DNA gene to detect is grafted on the surface. The studied solution, containing DNA strands marked by fluorescence, is deposited on the chip. There is a hybridization between the DNA at the surface and the target gene if the latter is present in the solution. The pixel's surface becomes fluorescent. The determination of the "genetic map" of the solution is then performed after rinsing by an optical scan of the whole chip.

Actually, the main limitation of the chips concerns their viability, as the hybridization's efficiency between grafted DNA and target genes is poor. This weak efficiency may come from a weak mobility of the grafted DNA strands, which does not allow the two complementary DNA strands to have a sufficient spatial mobility to hybridize. It is also possible to get a nonspecific physical or chemical adsorption of DNA strands in solution. An improvement of the DNA grafting at the surface should thus let the grafted DNA strands mobilize and avoid nonspecific adsorption.

Two ways of DNA grafting and neutron reflectivity are used to study the conformation of DNA strands at the surface. (1) DNA strands are linked to a protein that is first grafted on the surface. This allows the realization of dense DNA grafting, but the DNA strands are collapsed on the surface. (2) DNA strands are linked to the hydrophilic part of a diblock copolymer (hydrophilic/hydrophobic) adsorbed on the surface. The study of the conformation of the copolymer has shown good adsorption of the hydrophobic part and a correct dispersion of the hydrophobic part. This method is thus promising for the grafting of DNA strands.

## 7.10. Hydrogen as a tuning agent of the interlayer exchange coupling

V. Leiner,<sup>1</sup> K. Westerholt,<sup>2</sup> H. Zabel,<sup>2</sup> B. Hjörvarsson,<sup>3</sup>

<sup>1</sup>Institute Laue Langevin, France, <sup>2</sup>Ruhr-Universität Bochum, Germany, <sup>3</sup>Uppsala University, Sweden  
E-mail: [leiner@ill.fr](mailto:leiner@ill.fr)

The effect of interlayer exchange coupling on the ordering temperature of ultrathin magnetic layers has been explored for two systems: Ho/Y and Fe/V superlattices. In both cases, the exchange coupling can be modified and eventually removed by the introduction of hydrogen into the mediating nonmagnetic spacer layer. In the case of Ho/Y, we observed a drastic drop in the Ho Néel-temperature, from 103 K for coupled Ho blocks of 10 monolayer thickness to 74 K for isolated or uncoupled Ho blocks. In Fe/V superlattices, the incorporation of hydrogen changes the strength and sign of the exchange coupling constant. Again, we observed that the ordering temperature clearly depends on the strength of the exchange coupling in both the antiferromagnetically and the ferromagnetically coupled ranges of the phase diagram.

## 7.11. Real-time in-plane diffusion of Au nanoparticles in polymer thin films

S. Narayanan,<sup>1</sup> R. Guico,<sup>1</sup> D.R. Lee,<sup>1</sup> J. Wang,<sup>1</sup> A. Gibaud,<sup>2</sup> S.K. Sinha,<sup>3</sup>

<sup>1</sup>Argonne National Laboratory, USA, <sup>2</sup>University de Maine, France, <sup>3</sup>University of California (San Diego), USA  
E-mail: [sureshn@aps.anl.gov](mailto:sureshn@aps.anl.gov)

Dispersions of metal nanoparticles in polymeric matrices are of importance in the field of nanoscience. To study the dynamics and structural properties of highly diluted gold nanoparticles in ultrathin polymer films, we have developed a method involving resonance-enhanced grazing-incidence small-angle x-ray scattering (GISAXS) and diffuse scattering by nanocomposite thin films. The dynamics of the lateral diffusion of Au nanoparticles (2–3 nm in diameter) above the glass transition temperature (49°C) of the poly (tert-butyl acrylate) (PtBA) polymer has been studied in real time using resonance-enhanced GISAXS. The measurements have been carried out as a function of time in the temperature range of 60–80°C. The distribution in the lateral correlation of Au nanoparticles has been derived. The observed broadening of the distribution is attributed to the coalescing dynamics of Au nanoparticles in the polymer matrix. The in-plane diffusion related to the coalescing process is computed at different temperatures and is compared to the out-of-plane diffusion coefficients determined precisely.

Acknowledgments: The measurements were carried out at the 1-BM beamline at the APS. This work and the use of the APS are supported by the U.S. Department of Energy, under Contract No. W-31-109-ENG-38.

## 7.12. Neutron reflection study on the lipophilic-C<sub>60</sub> derivative at the air/water interface

U.S. Jeng,<sup>1</sup> T.L. Lin,<sup>1</sup> Z.-M. Lin,<sup>1</sup> Z.A. Chi,<sup>2</sup> .M.C. Shih,<sup>2</sup> L.Y. Chiang,<sup>3</sup> K. Shin<sup>4</sup>

<sup>1</sup>NTHU, Taiwan, <sup>2</sup>NCHU, Taiwan, <sup>3</sup>NTU, Taiwan, <sup>4</sup>NIST, USA

E-mail: [usjeng@mx.nthu.edu.tw](mailto:usjeng@mx.nthu.edu.tw)

We have studied a lipophilic-C<sub>60</sub> derivative synthesized recently for potential biomedical applications. The novel molecule, having three phospholipid-like tails chemically bonded on one olefinic moiety of the C<sub>60</sub> cage demonstrates a high compatibility with lecithin lipids. The reversible surface-pressure-area isotherms observed indicate that the lipophilic-C<sub>60</sub> derivatives can form Langmuir monolayers at the air/water interface. Using a Langmuir trough, we collected neutron reflection data for the lipophilic-C<sub>60</sub> spread and compressed these to several surface pressures at the air/water interface. For contrast variation, we used both D<sub>2</sub>O and H<sub>2</sub>O for the water substrate. The reflection result revealed a monolayer structure for the Langmuir film of lipophilic-C<sub>60</sub>. We extracted the structure information of the monolayer, including the density profile and area per molecule. For comparison, we also measured the lecithin lipids, which resemble the lipid tails of the lipophilic-C<sub>60</sub> derivatives.

## 7.13. SANS studies of polyelectrolyte multilayers on colloids and hollow capsules

I. Estrela-Lopis, S. Leoporatti, E. Donath, Leipzig University, Germany

E-mail: [esti@medizin.uni-leipzig.de](mailto:esti@medizin.uni-leipzig.de)

Oppositely charged polyelectrolytes (PE) can be assembled layer-wise on colloidal templates such as silica. When the silica core is dissolved in HF, hollow polyelectrolyte shells are obtained. Such hollow capsules may find a wide range of applications, e.g., as carrier systems for drug delivery.

In the present work, free PE layers (hollow capsules) were compared with the original supported PE layers on silica and polystyrene. Besides investigating the core removal, we also examined the influence of annealing at elevated temperatures and the salt concentration on the PE shell wall structure (thickness and density). Polyelectrolyte hollow shells were fabricated by templating monodisperse particles with pairs of poly(styrene sulfonate) (PSS) and poly(allyl amine hydrochloride) (PAH). Polyelectrolyte layers adsorbed on colloidal particles and free PE layer were investigated by means of small-angle neutron scattering at contrast-matching conditions. For the first time, the wall thicknesses of the polyelectrolyte coating on colloidal particles and hollow capsules were directly determined in an aqueous environment.

Pronounced periodic oscillations related to the latex particle size (small  $q$ ) and to the layer thickness (larger  $q$ ) have been seen. The scattering data could be fitted well taking into account resolution and polydispersity of particles if a step function density profile of the layer was used.

It was shown that the layers are rather dense with water content of 45%. The layer thickness and its density profile were independent on the curvature of the surface and dependent on the number of the adsorbed polyelectrolyte layers. The annealing of the hollow capsules lead to a decrease of thickness per one layer and the roughness.

## 7.14. Design and estimated performance of the SNS liquids reflectometer

<sup>1</sup>J.F. Ankner, Ch. Rehm, <sup>1</sup>R.L. Kellogg<sup>2</sup>

<sup>1</sup>Oak Ridge National Laboratory, USA, <sup>2</sup>Argonne National Laboratory, USA

E-mail: [jankner@anl.gov](mailto:jankner@anl.gov)

The liquids reflectometer at the Spallation Neutron Source (SNS), which will feature the world's highest peak neutron flux, will be equipped for both specular and off-specular reflectivity measurements. Design of the instrument is well underway, and procurement of the guide components and shielding has begun. Neutrons from a coupled 20-K supercritical hydrogen moderator will be delivered via a multichannel supermirror bender and tapered guide onto either a horizontal (liquid) or tilted (solid) surface. Collimating slits select the beam incident angle from a 0–5° vertical intensity distribution provided by the tapered guide. Bandwidth choppers and frame-overlap mirrors define a 3.75 Å wide wavelength band used in conjunction with the vertical intensity distribution to cover a broad Q range. The user will be able to collect data using either a two-dimensional position-sensitive detector or a single <sup>3</sup>He tube. With the SNS running at 1.4 MW, the instrument should be able to accumulate a complete specular reflectivity scan from D<sub>2</sub>O ( $R < 10^{-7}$ ,  $Q > 0.5 \text{ \AA}^{-1}$ ) in less than 10 min. We will describe the design of the SNS liquids reflectometer, compare it with a conventional instrument, and estimate its performance for more challenging problems, such as the study of time-dependent processes.

This work was supported by Contract No. US-DOE DE-AC05-960R22464.

## 7.15. SNS: The next generation neutron source

John F. Ankner (presenting author) and The SNS Instrument Systems Group, Oak Ridge National Laboratory, USA

E-mail: [jankner@anl.gov](mailto:jankner@anl.gov)

The Spallation Neutron Source, currently being constructed at Oak Ridge National Laboratory, will feature the highest peak neutron flux in the world when fully operational. We will describe the instruments currently under development. This work was supported by Contract No. US-DOE DE-AC05-960R22464.

## 7.16 Liquid surface/interface spectrometer at ChemMatCARS Synchrotron Facility at the Advanced Photon Sources

B. Lin,<sup>1</sup> M. Meron,<sup>1</sup> J. Gebhardt,<sup>1</sup> T. Graber,<sup>1</sup> P.J. Viccaro,<sup>1</sup> M. Schlossman<sup>2</sup>

<sup>1</sup>CARS, The University of Chicago, USA, <sup>2</sup>Department of Physics, University of Illinois at Chicago

E-mail: [binhua@cars.uchicago.edu](mailto:binhua@cars.uchicago.edu)

A liquid surface/interface spectrometer was successfully commissioned in the summer of 2002 at the ChemMatCARS synchrotron facility (Sector 15 Undulator beamline) at the Advanced Photon Source (Argonne National Laboratories). The spectrometer was designed and developed for the investigation of interfacial phenomena and properties of a wide variety of liquid systems, for example, (1) surfaces of complex fluids composed of polymers, lipids, liquid crystals, etc.; (2) interfaces between two immiscible liquids; (3) liquid metal-X interfaces; (4) superfluid helium surfaces; and (5) monolayers of amphiphilic phospholipid surfactants, protein-lipid mixtures, functional molecules, polymeric and biological macromolecules at the liquid-vapor or liquid-liquid interface. The high brilliance and wide x-ray energy range (5–30 keV) offered in this third generation insertion device beamline allows experimental measurements to probe surface/interfacial structures with much higher molecular resolution than is possible at a second generation synchrotron source.

We will present experimental results obtained during the commissioning period, including studies of liquid-liquid interfaces (Mark Schlossman, UIC), liquid metal-X interfaces (Stuart A Rice, Univ. of Chicago, and Peter Pershan, Harvard), and Langmuir monolayers (Schlossman and Ian Gentle, Univ. of Queensland, Australia). These results demonstrate the initial capabilities and potential broad applications of this new instrument in the field of liquid surface/interface studies.

\* \* \*

**SESSION NO. 8, 8:30 AM**  
**THURSDAY, 26 SEPTEMBER 2002**  
**LIQUIDS AND SOFT MATTER — I**  
**GRANLIBAKKEN CONFERENCE CENTER LAKE-BAY ROOM**

**8.1. High-energy X rays for the study of solid/liquid interfaces (Invited)**

H. Reichert, Max-Planck-Institut fuer Metallforschung, Germany  
E-mail: [reichert@dxray.mpi-stuttgart.mpg.de](mailto:reichert@dxray.mpi-stuttgart.mpg.de)

Most commonly, interfaces and surfaces are studied in surface scattering geometries—Grazing Angle Diffraction (GAD) and Crystal Truncation Rod Diffraction (CTRD)—at typical photon energies around 10 keV. These techniques are not applicable in the case of deeply buried interfaces for several reasons: Conventional x-ray scattering geometries are unable to separate the scattering signals from structurally modified thin layers at an interface from the large background of bulk-like scattering signals. Another problem is the strong absorption of the incoming and scattered beams within the solid and the liquid, which produce very weak scattering signals on top of a large background from the penetrated solid.

New techniques using high-energy photons in a high-resolution setup allow resolution of most of these problems. For a case study, we have used this technique to probe the interfacial liquid structure factor. We found strong experimental evidence for a profound modification of the interfacial liquid structure factor parallel and perpendicular to the interface in Pb(liq.)/Si(100). Such modifications have long been expected from simulations and are now experimentally accessible.

**8.2. Capillary waves on water**

C. Gutt,<sup>1</sup> M. Tolan,<sup>1</sup> T. Ghaderi,<sup>1</sup> A. Madsen,<sup>2</sup> T. Seydel,<sup>3</sup> V. Chamard,<sup>1</sup>  
<sup>1</sup>Univ. Dortmund, Germany, <sup>2</sup>ESRF, France, <sup>3</sup>ILL, France  
E-mail: [gutt@physik.uni-dortmund.de](mailto:gutt@physik.uni-dortmund.de)

Water is the most important liquid in nature. Although liquid water has been the focus of intense research for a long time, a coherent picture of its physical properties is still missing. In this context, most scattering experiments focussed on the bulk properties of water and ice, while only a few investigated its surface. Here, one of the most remarkable experimental results may be the finding of a q-dependent surface tension [1]. We studied the static and dynamic properties of the surface of liquid water from room temperature down to the supercooled state. X-ray reflectivity measurements have been performed in order to investigate the static properties of the surface capillary waves. For the first time, we observed propagating capillary waves on a liquid surface with x-ray correlation spectroscopy. Again, the measurements covered a broad temperature region, down to the supercooled state, where capillary waves are still present on the water surface.

[1] C. Fradin et al., Nature 403, 871 (2000).

### 8.3. X-ray photon correlation spectroscopy on polymer films with molecular weight dependence

H. Kim,<sup>1</sup> A. Rühm,<sup>2</sup> L. Lurio,<sup>3</sup> J. Basu,<sup>1</sup> J. Lal,<sup>4</sup> S. Mochrie,<sup>5</sup> S.K. Sinha,<sup>1</sup>

<sup>1</sup>University of California (San Diego), USA, <sup>2</sup>Max-Planck-Institut für Metallforschung, Germany,

<sup>3</sup>Northern Illinois University, USA, <sup>4</sup>Argonne National Laboratory, USA, <sup>5</sup>Yale University, USA

E-mail: [hjk@physics.ucsd.edu](mailto:hjk@physics.ucsd.edu)

We have applied x-ray photon correlation spectroscopy (XPCS) to study the dynamics of surface fluctuations in thin supported polystyrene films as a function of wave vector, temperature, film thickness, and molecular weight. Molecular weights, ranging from 30,000 to 650,000, were used in the study. Lateral length scales probed are at least ten times smaller than those accessible in conventional dynamic light scattering. Good agreement between the experimental results and conventional theory permits us to determine the film viscosity. The comparison between the values of the viscosity obtained from these data with those of bulk polystyrene will be discussed.

### 8.4. Real time measurements of nanoparticle diffusion in ultrathin polymer films using x-ray standing waves

R.S. Guico,<sup>1</sup> S. Narayanan,<sup>1</sup> J. Wang,<sup>1</sup> K. Shull,<sup>2</sup>

<sup>1</sup>Argonne National Laboratory, USA, <sup>2</sup>Northwestern University, USA

E-mail: [guico@aps.anl.gov](mailto:guico@aps.anl.gov)

Polymer/metal nanocomposites have emerged as an important research area due to their practical and fundamental significance in recent years. They have become model systems for studying nanoparticle structure and dynamics, especially in confined geometries. While recent work in this field has focused on metallic interactions with diblock copolymer templates for construction of devices such as nanowires, much can still be learned from the diffusive properties of nanoparticles in homopolymer matrices. In the current work, we have measured the diffusion of gold nanoparticles in ultrathin polymer films in real time as the samples are annealed above the polymer glass transition temperature ( $T_g$ ). The profile of the gold distribution perpendicular to the polymer film surfaces and interfaces was precisely determined using total external reflection x-ray standing waves (TER-XSWs). The TER-XSW method was used previously to locate a heavy atom marker layer in organic films with angstrom spatial resolution. In this study, the gold mobility was measured in situ and in a time-resolved manner. Since we are interested in probing the single-particle dynamics and mobility before the nanoparticles coalesce, TER-XSWs become necessary in order to measure the gold distribution over short diffusion distances. These distributions were used to obtain effective diffusion coefficients at various annealing temperatures. Molecular weight and thickness effects on the gold nanoparticle diffusive properties have also been investigated.

This work and use of the Advanced Photon Source were supported by the U.S. Department of Energy, Office of Science, Office of Basic Energy Sciences, under Contract No. W-31-109-Eng-38.

## 8.5. Lipid discrimination of antimicrobial peptides studied by GIXD

F. Bringezu, University of Leipzig, Germany, G. Brezesinski, Max Planck Institute of Colloids and Interfaces, Germany, A. Waring, UCLA, USA, R.I. Lehrer, UCLA, USA  
E-mail: [brif@medizin.uni-leipzig.de](mailto:brif@medizin.uni-leipzig.de)

Antimicrobial peptides are increasingly recognized as compartments of the innate defense system of animals and plants because they can kill bacteria by cell membrane permeation. Differing lipid compositions of bacterial and eukaryotic cell membranes indicate the specific interaction between peptides and lipids as key steps in the mode of action and cell recognition.

Our study is focused on a novel antimicrobial peptide from hemocytes of a tunicate, *halocynthia aurantium*. The lipid/peptide systems were studied in monolayers at the air/water interface by means of pressure-area isotherms. The introduction of a fluorescent label in the peptide allowed the direct visualization of the interaction. Grazing incidence x-ray diffraction measurements (GIXD) provided information about the change in the lipid structure on peptide adsorption and incorporation into the layer.

GIXD measurements on pure DPPG monolayers revealed a condensed phase with tilted chains in an orthorhombic 2D lattice ( $L_{2d}$ ). Increasing pressure leads to the hexatic LS phase with nontilted molecules. After adsorption of Cynthaurine, the isotherms are shifted to larger area values, suggesting an incorporation of the peptide into the lipid layer. GIXD measurements revealed a larger chain tilt in the  $L_{2d}$  phase and an increased transition pressure, indicating a disturbance of the chain packing induced by the peptide adsorption. The largest influence on the structures was observed in a pressure region that is relevant in vivo. Studies on DPPE/DPPS monolayers showed no influence on the lipid chain lattice, hence a specific interaction of Cynthaurine with lipid head groups rather than an unspecific adsorption/incorporation must be assumed.

\* \* \*

**SESSION No. 9, 11:00 AM**  
**THURSDAY, 26 SEPTEMBER 2002**  
**LIQUIDS AND SOFT MATTER — II**  
**GRANLIBAKKEN CONFERENCE CENTER LAKE-BAY ROOM**

**9.1. Surface dynamics of polymer films studied via XPCS (Invited)**

S.G.J. Mochrie,<sup>1</sup> H. Kim,<sup>2</sup> S.K. Sinha,<sup>2</sup> J. Lal,<sup>3</sup> J. Basu,<sup>2</sup> A. Ruehm,<sup>4</sup> L.B. Lurio,<sup>4</sup>

<sup>1</sup>Yale University, USA, <sup>2</sup>University of California (San Diego), USA, <sup>3</sup>Argonne National Laboratory, USA,

<sup>4</sup>MIT, USA

E-mail: [simon.mochrie@yale.edu](mailto:simon.mochrie@yale.edu)

X-ray photon correlation spectroscopy (XPCS) is an emerging method for studying the slow dynamics of strongly scattering condensed matter. This talk will, first, review the principles of XPCS using XPCS measurements on a colloidal suspension as a illustration of the technique. The talk will then describe XPCS measurements of the dynamics of supported polystyrene films. Specifically, experiments will be described that determine the relaxation rates of surface height fluctuations (capillary waves) as a function of the capillary wave vector, film thickness, and temperature. For the ranges studied—temperatures between 150 and 170°C, film thicknesses between 80 and 300 nm, and wave vectors between 0.001 and 0.01 inverse nm—good agreement was found between the measured capillary dynamics and the hydrodynamic theory of overdamped capillary waves on the surface of thin films. These observations will be discussed in the context of recent reports that the surface of polymer films remains "liquid-like" to temperatures tens of degrees below the bulk glass transition temperature. Prospects for further XPCS studies of capillary and thin film dynamics will also be mentioned.

**9.2. Dynamics of a liquid crystal surface near the Nematic-to-Smectic A transition: A critical scattering study applying coherent X rays**

A. Madsen,<sup>1</sup> G. Grübel,<sup>1</sup> J. Als-Nielsen,<sup>2</sup>

<sup>1</sup>ESRF, France, <sup>2</sup>Niels Bohr Institute, Denmark

E-mail: [amadsen@esrf.fr](mailto:amadsen@esrf.fr)

The dynamics and ordering of a liquid crystal (8OCB) is investigated by x-ray scattering from the free surface. The Smectic A order that develops when the phase transition temperature  $T_{NA}$  is approached is probed by x-ray reflectivity applying a noncoherent beam. The results confirm that the Smectic order correlation length diverges at the transition as  $t^{-\nu}$  where  $t$  is the reduced temperature. In the direction parallel to the 8OCB molecules,  $\nu_{\parallel} = 0.70$ , while  $\nu_{\perp} = 0.58$  for the perpendicular direction.

The dynamics of the free 8OCB surface is probed by X-ray Photon Correlation Spectroscopy (XPCS) applying a coherent x-ray beam. The surface dynamics are governed by capillary waves that decorate the surface depending on the surface tension and the viscosity. The viscosity of a Nematic liquid is anisotropic and can be described by three viscosity coefficients  $\eta_{1-3}$ . The Smectic phase can be thought of as a stack of 2D liquid layers with solid-like ordering normal to the layers. This is reflected by the dynamic behavior of the liquid crystal surface near the N-to-SmA transition, where only the viscosity coefficient  $\eta_3$  diverges. We demonstrate that it is possible to derive the critical exponent  $\beta$  of  $\eta_3$  by XPCS and find that  $\beta = 0.94$ . The result is in contradiction to previously published light scattering results but in excellent agreement with the theoretical prediction  $\beta = 3\nu_{\parallel} - 2\nu_{\perp}$ .

This experiment shows that with a brilliant x-ray source, it is possible to simultaneously carry out static and dynamic investigations on the same system. In particular, our results illustrate that the combination of noncoherent and coherent critical scattering is very useful in the study of phase transitions.

### 9.3. X-ray and neutron surface investigations of highly viscous liquids

T. Seydel,<sup>1</sup> A. Madsen,<sup>2</sup> M. Tolan,<sup>3</sup> B.M. Ocko,<sup>4</sup> J. Major,<sup>5</sup>

<sup>1</sup>ILL, France, <sup>2</sup>ESRF, France, <sup>3</sup>Univ. Dortmund, Germany, <sup>4</sup>BNL, USA, <sup>5</sup>MPI Stuttgart, Germany

E-mail: [seydel@ill.fr](mailto:seydel@ill.fr)

While surfaces of liquids with low viscosity as well as surfaces of thin polymer films have already been extensively investigated using x-ray and neutron techniques, very little is known about the surfaces of highly viscous and supercooled liquids or glasses and their glass transition. Recently, it has become possible to directly observe overdamped capillary waves on surfaces of supercooled glycerol and poly(propylene glycol) in a wide temperature range by x-ray photon correlation spectroscopy (XPCS) in a grazing incidence scattering geometry. XPCS probes capillary waves in the most direct and unambiguous way on length scales that are not accessible by light scattering. The relation between overdamped capillary wave dynamics and the capillary wave-induced rms roughness as seen by “incoherent” x-ray scattering is not yet well understood. The rms roughness observed by x-ray scattering is significantly smaller than predicted by the standard capillary waves theory. However, with respect to the interpretation of the x-ray reflectivity data, some questions remain open. In particular, it is not clear yet whether a bulk layering due to correlations induced by the H bonds of the network glass glycerol affects the surface. Furthermore, the slow evolution of highly viscous liquids renders the experiments sensitive to different experimental time scales. X-ray and neutron reflectivity data as well as diffuse scattering and XPCS measurements on prototypical systems will be discussed in the context of the capillary waves model.

[1] T. Seydel, A. Madsen, M. Tolan, G. Gruebel, and W. Press; Phys. Rev. B 63, 073409 (2001).

[2] T. Seydel, M. Tolan, B.M. Ocko, O.H. Seeck, R. Weber, E. DiMasi, and W. Press; Phys. Rev. B. 65, 184207 (2002).

### 9.4. Thin-film polymers used as x-ray waveguides (Invited)

T. Salditt, Universität des Saarlandes, Germany

E-mail: [Salditt@mx.uni-saarland.de](mailto:Salditt@mx.uni-saarland.de)

We will present recent work on thin -film nanostructures that act as x-ray waveguides. In contrast to previous inorganic nanostructures, these systems consist of low-density self-assembled macromolecular samples imbedded in high-density metal layers, which are evaporated or sputtered onto the macromolecular entity. At precise angles x-ray resonances can be excited, leading to local field enhancement of up to two orders of magnitude (calculated). Structural analysis with enhanced signal to noise ratio can then be carried out in the geometry of grazing incidence diffraction. A specific example of phospholipid membranes is presented, and general aspects of such x-ray waveguide structures are discussed, also in view of 2D waveguide structures.

\* \* \*

**SESSION No. 10, 7:30 P.M.**  
**THURSDAY, 26 SEPTEMBER 2002**  
**MAGNETIC FILMS — II**  
**GRANLIBAKKEN CONFERENCE CENTER LAKE-BAY ROOM**

**10.1. Supermatrix formalism to model off-specular neutron scattering (Invited)**

B.P. Toperverg, FZ Jülich, Germany

E-mail: [b.toperverg@fz-juelich.de](mailto:b.toperverg@fz-juelich.de)

Supermatrix formalism (SMF) is developed to describe all four components of polarized neutron reflectivity from arbitrary noncollinear magnetization arrangements in layered systems at arbitrary orientation between the directions of incident polarization and polarization analysis. This allows the reconstruction of complex profiles of the mean magnetization vector averaged over the lateral projection of the neutron coherence length. Lateral irregularities (i.e., interfacial roughness, magnetic domains, and artificial lateral patterns with dimensions smaller than this coherence length projection) scatter neutrons into off-specular directions. This scattering is used to retrieve corresponding information on the system. However, it also carries a signature of the mean layer magnetization as soon as incident and scattered neutron waves are reflected and refracted in the mean layer potential. That is why neither specular reflectivity nor off-specular scattering alone is sufficient to refine a model, and both of them are to be evaluated simultaneously over a broad range of incoming and outgoing wave vectors at various directions of the polarization vectors. This requirement is mostly met by the Supermatrix Formulation of the Distorted Wave Born Approximation (SMF-DWBA). Examples of application of SMF-DWBA are presented, its limitations are examined, and alternative approaches are indicated. In particular, the super-recursion routine generalizing known as the Parratt approach, for the case of spin 1/2 particle, is considered as an alternative to SMF.

**10.2. Mapping magnetic disorder in magnetic multilayers (Invited)**

S. Langridge,<sup>1</sup> R.M. Dalgliesh,<sup>1</sup> C.H. Marrows,<sup>2</sup> B.J. Hickey,<sup>2</sup> M. Ali,<sup>2</sup> A.T. Hindmarch,<sup>2</sup>

<sup>1</sup>Rutherford Appleton Laboratory, United Kingdom, <sup>2</sup>University of Leeds, United Kingdom

E-mail: [s.langridge@rl.ac.uk](mailto:s.langridge@rl.ac.uk)

It is now well known that magnetic multilayers comprising 3D ferromagnetic layers interleaved with nonmagnetic spacers exhibit giant magnetoresistance (GMR). The change in resistivity arises from the spin-dependent scattering of the conduction electrons, which depends not only on the magnetic moment alignment but also on the interfacial disorder and the details of the magnetic domain structure. Polarised neutron reflectometry (PNR) is ideally suited to the study of such systems and to the study of the magnetic disorder.

In this talk, we shall use PNR to quantitatively study the magnetic domain structures in exchange-biased [1] GMR multilayers. An analysis of both the specular and off-specular data provides a valuable insight into the magnetic domain structures (both in-plane and out-of-plane) that may play a role [2,3] in the magnitude of the experimentally observed exchange bias.

[1] W. H. Meiklejohn and C. P. Bean, Phys. Rev. 102, 1413 (1956).

[2] A. P. Malozemoff, Phys. Rev. B 35, 3679 (1987).

[3] D. Mauri, H. C. Siegmann, P. S. Bagus, and E. Kay, J. Appl. Phys. 62, 3047 (1987).

### 10.3. Polarized neutron reflectivity studies on laterally structured stripe arrays

K. Theis-Bröhl, V. Leiner, T. Schmitte, H. Zabel, Ruhr-Universität Bochum, Germany

E-mail: [k.theis-broehl@ruhr-uni-bochum.de](mailto:k.theis-broehl@ruhr-uni-bochum.de)

Laterally structured magnetic stripes and dots are important components of future magnetic storage elements. New insight into the remagnetization processes of lateral arrays beyond the characterization by other methods, such as the magneto-optical Kerr effect, can be gained by PNR. Analysis of the magnetization in reciprocal space filters out correlation effects and therefore is suitable for studying interaction effects. Application of neutron scattering methods to nanometer- and micrometer-scale lateral structures is, however, a challenging task. First, neutron scattering requires a large area of a homogeneously structured pattern. Second, the repeat distance is often unfavorable for work at small angles close to total reflectivity. We performed reflectivity experiments on stripe arrays in the nanometer and micrometer range and demonstrate that the magnetization reversal of a laterally structured film can be probed using polarized neutron reflectivity in the off-specular regime. The magnetization reversal process was studied under the condition of specular reflectivity and at off-specular Bragg-peaks in  $Q_x$  direction for different tilt angles. The non-spin flip and the spin-flip cross sections were determined in order to discriminate between a magnetization reversal by domain formation and propagation and by rotational processes. We studied two types of stripe arrays prepared by different methods. Magnetization reversals for different field directions were performed at the two types of samples and are discussed and compared to MOKE and SQUID studies of the same systems. We acknowledge funding by DFG-SFB 491 and by BMBF 032AE8BO.

### 10.4. Self-assembled nanomaterials: magnetic nanoparticles in copolymer films studied by off-specular neutron scattering

V. Lauter-Pasyuk,<sup>1</sup> H. Lauter,<sup>2</sup> G. Gordeev,<sup>3</sup> P. Müller-Buschbaum,<sup>4</sup> B.P. Toperverg,<sup>5</sup> W. Petry,<sup>4</sup>

<sup>1</sup>TU München c/o ILL, France, <sup>2</sup>Institute Laue Langevin, France, <sup>3</sup>PNPI, Russia, <sup>4</sup>TU München, Germany, <sup>5</sup>FZ Jülich, Germany

E-mail: [vlauter@ill.fr](mailto:vlauter@ill.fr)

For the first time, a magnetic response was obtained from a self-assembled composite lamellar nanomaterial. The pure copolymer film showed an unusual structure with a perpendicular to the surface orientation of the lamellae. This is a new phenomenon because up to now this orientation was only obtained on specially prepared surfaces. After the incorporation of nanoparticles into the copolymer matrix, the system switched to a lamellar structure parallel to the surface. The full quantitative analysis of both specular reflection and off-specular scattering of the complete two-dimensional intensity map allows deducing the layer-by-layer configuration through the multilayer stack, as well as the lateral structure and the magnetic particles' distribution within the plane of the layers. The analysis of the off-specular scattering comprises Bragg-sheet scattering, Yoneda scattering, and their interference in the dynamical range.

Recent achievements in the synthesis of novel artificially structured systems, copolymer—nanoparticle composites, are presented. The nanocomposite was designed using a template matrix formed with symmetric P(S-b-MMA<sub>d</sub>) diblock copolymers. These copolymers spontaneously self-assemble during annealing into a regular lamellar structure. Magnetite nanoparticles ( $\text{Fe}_3\text{O}_4$ ) have a selective affinity to one of the blocks (PS) and self-assemble within the PS-lamellae of the copolymer film during annealing. We succeeded to incorporate nanoparticles up to 8% of the volume fraction. Even for a high concentration the particles stay included in the film and the lamellar structure is not destroyed.

\* \* \*

**SESSION NO. 11, 8:30 A.M.**  
**FRIDAY, 27 SEPTEMBER 2002**  
**LIQUIDS AND SOFT MATTER — III**  
**GRANLIBAKKEN CONFERENCE CENTER LAKE-BAY ROOM**

**11.1. X-ray and neutron surface studies of cholera toxins interaction with lipid monolayer at the air/water interface**

J. Majewski,<sup>1</sup> T. Kuhl,<sup>2</sup> G. Smith<sup>3</sup> K. Kjaer,<sup>4</sup> S. Satija<sup>5</sup>

<sup>1</sup>Los Alamos National Laboratory, USA, <sup>2</sup>University of California Davis, <sup>3</sup>Oak Ridge National Laboratory,

<sup>4</sup>Risoe National Laboratory, Denmark, <sup>5</sup>National Institute of Standards and Technology

E-mail: [jarek@lanl.gov](mailto:jarek@lanl.gov)

Cholera is caused by a comma-shaped bacterium, *vibrio cholerae*. The bacteria multiply in the intestine and produce a hexameric AB<sub>5</sub> structured toxin. This toxin binds specifically to glycolipid (GM<sub>1</sub>) constituents of (epithelial) cell membranes through the B<sub>5</sub> pentameric unit. The A fragment then penetrates through the membrane and irreversibly activates the G proteins of epithelial cells. This results in a life-threatening influx of sodium and water into the gut lumen [1,2]. Using in situ surface-sensitive x-ray and neutron scattering methods, the time evolution of the toxin's assault on a model mixed monolayer of ganglioside GM<sub>1</sub> and dipalmitoyl-phosphatidylethanolamine (DPPE) was determined. Both in-plane and out-of-plane 2D packing alterations of this lipid monolayer structure were followed upon protein binding. These structural studies enabled the protein's position within and effect on the lipid layer to be directly measured, enriching our understanding of bacterial intoxication mechanisms and membrane-protein structure function properties in general.

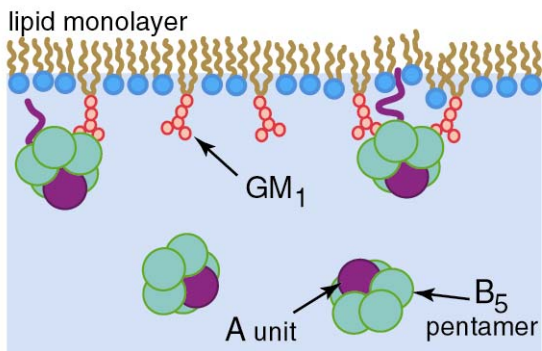


**Figure 1** Schematic of the model membrane system studied with x-ray and neutron scattering.

[1] Ribi, H.O., et al., Science 239, 1272 (1988)

[2] Zhang, R.-G., et al., JMB 25,1 250 & 563 (1995)

## 11.2. Structure of brushite/water interface

J. Arsic, D. Kaminski, P. Poodt, E. Vlieg, University of Nijmegen, Netherlands  
E-mail: [jelena@sci.kun.nl](mailto:jelena@sci.kun.nl)

Bioceramic materials are in clinical use worldwide, and their applications are increasing in many specialties: from dentistry to orthopedic and plastic surgery. Brushite,  $\text{CaHPO}_4 \cdot 2\text{H}_2\text{O}$ , is of particular interest. This crystal is one of the major components of kidney stones and has a wide use as a coating for body implants. From a fundamental point of view, brushite is considered as the model system for biomineralisation. It grows easily from solution in a plate-like morphology and contains water layers incorporated in its structure. The surface is highly hydrated. Impurities are known to affect the growth of various faces. Our interest in brushite arises from our study of solid/liquid interfaces. Knowledge of the atomic structure of a solid/liquid interface is important in order to understand the different processes occurring at the interface, such as crystal growth, lubrication, or catalysis. Owing to the truncation of the surface, the atomic structure can differ from the bulk crystallographic structure. Similarly, the liquid near the interface may differ from a bulk liquid, because it is influenced by the periodic potential of the crystal surface and is expected to show more ordering than in the bulk. In the case of crystal growth, this will influence parameters such as incorporation of impurities, the stability of a surface, the growth speed, and the binding of a molecules to the surface. Using surface x-ray diffraction, we have determined the atomic structure of the brushite (010)/water interface. Besides the surface termination, we have also determined the strong ordering of the liquid near the interface.

## 11.3. In situ x-ray standing wave profiling of biomolecular adsorption at a charged interface

M.J. Bedzyk, K. Zhang, J. Libera, H. Cheng, M. Olvera de la Cruz, L. Cao, Northwestern University, USA  
E-mail: [bedzyk@northwestern.edu](mailto:bedzyk@northwestern.edu)

An important scientific challenge is understanding and controlling the assembly of biomolecules. Since most proteins, nucleic acids, and biomembranes are charged, it is essential to include electrostatic interactions in determining biological structures and processes. The interplay between short- and long-range electrostatic interactions in the self-assembly of structures, however, is poorly understood. To this end, we are studying the adsorption of negatively charged RNA (mercurated-poly-U) to a negatively charged (hydroxylated  $\text{SiO}_2$ ) surface via short-range electrostatic bridging with divalent cations ( $\text{Zn}^{2+}$ ). The Hg and Zn distribution profiles along the surface normal direction are measured by long-period x-ray standing waves (XSW) and compared to theoretical modeling that considers thermodynamics of the system, including short-range and long-rang electrostatics. The XSW is generated by total external reflection [1,2] from a Si/Mo multiple layer substrate. By probing the Zn  $K\alpha$  and Hg  $L\alpha$  fluorescence yield intensity under XSW, we determine the  $\text{Zn}^{2+}$  ion and poly-U z-distribution profiles above the interface as a function of  $\text{ZnCl}_2$  concentration. At certain  $\text{Zn}^{2+}$  concentrations, we observe changes in the poly-U profile that strongly suggest adsorption via ion bridging. The  $\text{Zn}^{2+}$  distribution above the interface also shows interesting changes. These results demonstrate how XSW can be used to determine the in situ adsorption z-distribution profile for poly-ions at a charged x-ray reflecting surface.

- [1] M.J. Bedzyk, G.M. Bommarito, M. Caffrey, and T.L. Penner, *Science* 248, 52 (1990).  
[2]. J. Wang, M. Caffrey, M.J. Bedzyk, and T.L. Penner, *Langmuir* 17, 3671-3681 (2001).

#### 11.4. Thermal denaturation of interfacial protein layers

J.W. White,<sup>1</sup> M.J. Henderson,<sup>1</sup> S.A. Holt,<sup>2</sup>

<sup>1</sup>Australian National University, Australia, <sup>2</sup>ISIS, United Kingdom

E-mail: [jww@rsc.anu.edu.au](mailto:jww@rsc.anu.edu.au)

We report for the first time measurements of the evolving structures in the denaturation of b lactoglobulin and lysozyme at an air-water interface. The incipient denaturation shown previously [1] for myoglobin is also studied for these molecules at room temperature, and denaturation is provoked by increasing the temperature of the solutions progressively to 75°C. The change in the adsorbed protein layer thickness, its scattering length density, and density distribution perpendicular to the surface as a function of increased temperature are reported and the data analysed in terms of a two-state model for the denaturation process to give thermodynamic information on the surface contribution to the denaturation. These measurements are relevant to an understanding of the way in which proteins at interfaces act as templates, for example, in biomineralisation.

[1] S.A. Holt, D.J. McGillivray, S. Poon, J.W. White, J. Phys. Chem. B. 2000, 104, 7431-7438.

#### 11.5. X-ray and neutron scattering studies of mesoporous silicate films

S.A. Holt, ISIS, United Kingdom, J.L. Ruggles, University of Queensland, Australia, J.W. White, Australian National University, Australia

E-mail: [S.A.Holt@rl.ac.uk](mailto:S.A.Holt@rl.ac.uk)

Mesoporous silicated thin films self assemble at interfaces from the appropriate solutions at room temperature. The film structure is determined by the liquid crystal phase of the templating surfactant. Constrained refinement of x-ray and neutron specular reflectometry has proved to be a valuable tool to study to a high precision the self-assembly in this soft condensed matter system. Film formation consists of a long induction time (greater than three hours) followed by a rapid growth phase. During induction, the initial surfactant surface excess develops into a structure about 9 layers thick, then the growth process takes over and hundreds of layers assemble in the next 30 to 60 minutes. The in-plane structure and interfacial correlations can best be probed in situ by grazing incidence diffraction (GID) and off-specular scattering. With the GID configured at a synchrotron with an image plate detector, it is possible to cover a wide region of Q space with exposure times of 10 seconds or less, as seen below. This demonstrates the flexibility of the silica framework in that the film structure is altered in the same manner as the surfactant phase is by temperature. Analysis of the off-specular and grazing incidence neutron diffraction is currently underway.

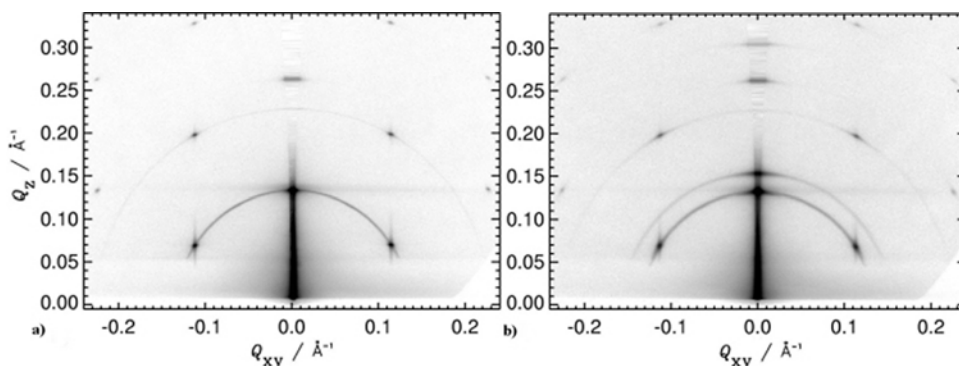


**Figure 1** X-ray diffraction, incident angle 0.59°, from C<sub>18</sub>TABr templated film at the air/water interface: (a) 65°C and (b) 25°C.

\* \* \*

**SESSION NO. 12, 10:40 AM**  
**FRIDAY, 27 SEPTEMBER 2002**  
**NEW METHODS — DIRECT INVERSION**  
**GRANLIBAKKEN CONFERENCE CENTER LAKE-BAY ROOM**

**12.1. Solving the inverse problem of surface x-ray diffraction (Invited)**

D.K. Saldin, University of Wisconsin-Milwaukee, USA  
E-mail: [dkaldin@uwm.edu](mailto:dkaldin@uwm.edu)

The fundamental difficulty in directly inverting surface x-ray diffraction (SXR) data for structure solution is the well-known phase problem that has also plagued other fields, such as protein crystallography. In SXR, the measured intensities arise from a sum of the known bulk and the unknown surface structure factors. In other branches of crystallography, this is known as the structure completion problem, and also has some analogy to the problem of holography. We will show how information about the bulk structure, combined with an iterative algorithm that alternately satisfies constraints in real and reciprocal space, enables the direct recovery of the electron density distribution in a surface unit cell, even when the diffraction pattern contains contributions from multiple domains.

**12.2. Phase determination and direct inversion in specular neutron reflectometry (Invited)**

C. Majkrzak, N.F. Berk, National Institute of Standards and Technology, USA  
E-mail: [charles.majkrzak@nist.gov](mailto:charles.majkrzak@nist.gov)

Exact methods for the determination of the complex reflection amplitude in specular neutron reflectometry make it possible to obtain a unique scattering length density (SLD) depth profile by first-principles inversion. These techniques, which involve the use of reference films or substrates, are reviewed. In addition to the direct determination of the depth profile, important diagnostic information regarding sample film homogeneity, as well as a measure of the resolution in the SLD profile, can be deduced from the imaginary and real components of the reflection amplitude, respectively. A discussion of these analytical techniques, including some specific illustrative examples, are presented.

\* \* \*

# **AUTHOR INDEX**



## A

Adelmann, Christoph: 5.4  
Ali, Mannan: 10.2  
Als-Nielsen, Jens: 9.2  
Anderson, C.: 1.2  
Ankner, John Francis: 7.14, 7.15  
Arendt, P.N.: 2.1  
Arsic, Jelena: 11.2  
Arvanitis, Dimitri: 4.3  
Aubertine, Daniel B.: 5.2  
Auciello, O.: 3.1  
Ay, Murat: 4.19

## B

Bader, Samuel D.: 6.5  
Bastie, Pierre: 4.5  
Basu, Jaydeep: 8.3, 9.1  
Bauer, G.: 4.6  
Becker, Hans-Werner: 4.1  
Bedzyk, Michael J.: 11.3  
Bellet-Amalric, Edith: 5.4  
Berk, Norman F.: 12.2  
Birch, Jens: 4.11  
Borchers, Julie A.: 2.3  
Botez, C.E.: 3.2  
Boué, François: 7.9  
Bowers, James: 7.3  
Brezesinski, Gerald: 7.4, 7.8, 8.5  
Bringezu, Frank: 7.4, 7.8, 8.5  
Brookes, Nick B.: 4.15, 6.3  
Bruegemann, Lutz: 4.10

## C

Cao, Lixin: 11.3  
Casalis, Loredana: 7.2  
Chamard, Virginie: 4.5, 5.4, 7.7, 8.2  
Cheng, Hao: 11.3  
Chi, Zhau Ann: 7.12  
Chiang, Long Y.: 7.12  
Chyi, J.-I.: 7.5  
Clemens, Bruce M.: 3.5  
Clemens, H.: 4.6  
  
Conrad, E.: 3.2  
Cousin, Fabrice: 7.9

## D

Dalgliesh, Robert M: 10.2  
Danisman, Mehmet F.: 7.2  
Daudin, Bruno: 5.4  
deJeu, Wim: 7.6

Devon, Mike: 6.2  
Dhesi, Sarnjeet: 4.15, 6.3  
Dietsch, Rainer: 4.10  
Ding, Junqi: 7.4  
Dolino, Gerard: 4.5  
Donath, Edwin: 7.13  
Dosch, H.: 1.2  
Dura, J.A.: 2.1

## E

Eastman, J. A.: 3.1  
Elkaim, Eric: 4.5  
Elliott, W. C.: 3.2  
Estrela-Lopis, Irina: 7.13

## F

Farmer, John: 4.16  
Felcher, Gian P.: 1.2, 4.16, 6.5  
Ferrero, Claudio: 4.5  
Fitzsimmons, M.R.: 1.1, 2.1  
Fong, D. D.: 3.1  
Frahm, R.: 4.9  
Fritsche, Helmut: 1.1  
Fritzsche, H.: 2.1  
Fullerton, Eric E.: 2.3, 6.1, 6.4  
Fuoss, P. H.: 3.1

## G

Gebhardt, J.: 7.16  
Ghaderi, Tuana: 8.2  
Gibaud, Alain: 7.11  
Goedkoop, Jeroen B.: 4.15, 6.3  
Gomozov, Valeriy: 4.14  
Gordeev, G.: 10.4  
Goyette, Rick: 4.16  
Graber, T.: 7.16  
Grenzer, Jörg: 4.4  
Grotkopp, Ingo: 3.4, 7.7  
Groves, J.R.: 2.1  
Grübel, Gerhard: 9.2  
Guico, R.: 7.11, 8.4  
Gutt, Christian: 8.2

## H

Habicht, K.: 1.2  
Hahlin, Anders: 4.3  
Han, Sang-Wook: 4.16  
Hashizume, H.: 4.2, 4.18  
Haskel, Daniel: 4.2  
Hellwig, Olav: 2.3, 4.1, 6.4

Henderson, M.J.: 11.4  
Hickey, Bryan J: 10.2  
Hindmarch, Aidan T: 10.2  
Hjörvarsson, Björgvin: 4.11, 7.10  
Hoffmann, A.: 2.1  
Holt, Stephen A: 11.4, 11.5  
Holý, Václav: 5.4  
Hosoito, N.: 4.2, 4.18  
Hsu, C.-H.: 7.5  
Huang, J.C.A.: 4.7  
Hunter Dunn, Jonathan: 4.3

## I

Ianotta, Salvatore: 7.2  
Inaba, Katsuhiko: 5.3  
Ishiji, K.: 4.18  
Ito, Yoshiyasu: 5.3

## J

Jeng, U-Ser: 7.12  
Jiang, Jidong Samuel: 6.5

## K

Kaminski, Daniel: 11.2  
Kao, Chi-Chang: 6.5  
Karis, Olof: 4.3  
Keil, P.: 4.9  
Keller, T.: 1.2  
Kern, Brandon: 6.2  
Ketterson, J.B.: 4.16  
Kiehne, G.T.: 4.16  
Kim, Hyunjung: 7.6, 8.3, 9.1  
Kim, Sang-Koog: 4.17  
Kjaer, Kristian: 11.1  
Konovalov, Oleg: 7.1  
Koprinarov, Ivaylo: 6.2  
Kortright, J.B.: 4.17, 6.2, 6.4  
Krenn, H.: 4.6  
Ku, Z.A.: 4.7  
Kuhl, Tonya: 11.1

## L

Lal, Jyotsana: 8.3, 9.1  
Lambrea, Denitza: 7.6  
Landes, Brian: 6.2  
Langer, Juergen: 4.3  
Langridge, Sean: 10.2  
Lauriat, Jean-Pierre: 4.5  
Lauter, H.: 2.1, 2.2, 10.4

Lauter-Pasyuk, V.: 2.2, 10.4  
Le Bolloc'h, David: 4.5  
Lechner, Rainer T.: 4.6  
Lee, Chih-Hao: 4.7  
Lee, Dong Ryeol: 4.13, 7.11  
Lee, Hsin-Yi: 7.5  
Lee, Hyun Hwi: 5.5  
Lehrer, Robert I.: 8.5  
Leighton, C.: 2.1  
Leiner, V.: 2.1, 4.11, 4.12, 7.10, 10.3  
Leporatti, Stefano: 7.13  
Li, K.: 3.2  
Liang, K.S.: 5.5, 7.5  
Libera, Joseph: 11.3  
Lin, B.: 7.16  
Lin, Ming-Zhe: 4.7  
Lin, Tsang-Lang: 7.12  
Lin, Z.-M.: 7.12  
Liu, Kai: 2.1  
Lohner, Karl: 7.1  
Lott, Dieter: 4.6, 6.5  
Lu, E.: 3.2  
Lurio, Laurence: 8.3, 9.1  
Lyons, John: 6.2  
Lützenkirchen-Hecht, Dirk: 4.9

## M

Madsen, Anders: 8.2, 9.2, 9.3  
Majewski, Jaroslaw: 11.1  
Majkrzak, C.F.: 2.1, 2.3, 12.2  
Major, J.: 1.1, 1.2, 9.3  
Maletta, Hansjoerg: 4.3  
Malette, Henri: 5.4  
Marrows, Christopher H: 10.2  
Marshall, Ann F.: 5.2  
McIntyre, Paul C.: 5.2  
Menelle, Alain: 7.9  
Meron, M.: 7.16  
Metzger, Till H.: 3.3, 5.4  
Miceli, P.F.: 3.2, 4.16  
Miguel, Jorge: 4.15, 6.3  
Mihaylova, Milena: 7.6  
Milyaev, M.: 2.2  
Mitchell, Gary: 6.2  
Mochrie, Simon: 8.3, 9.1  
Mozelev, Alexander: 4.20  
Mueller, Martin: 3.4  
Munkholm, A.: 3.1  
Murphy, Bridget M: 3.4  
Murty, M.V. Ramana: 3.1  
Myagkov, Igor: 7.1  
Müller-Buschbaum, P.: 10.4

## N

Narayanan, Suresh: 7.11, 8.4  
Nefedov, A.: 4.19  
Nickel, Bert: 7.2  
Nogues, J.: 2.1  
Noh, D. Y.: 5.5, 7.5

## O

O'Donovan, Kevin V.: 2.3  
Ocko, B.M.: 9.3  
Ohkochi, Takuo: 4.2  
Okuda, H.: 4.18  
Olvera de la Cruz, Monica: 11.3  
Omote, Kazuhiko: 5.3  
Ozguven, Nevran: 5.2

## P

Panzer, Tobias: 4.4  
Peters, Joost F.: 4.15, 6.3  
Peterson, Brennan L: 3.5  
Petry, W.: 10.4  
Pietsch, Ullrich: 4.4  
Poodt, Paul: 11.2  
Press, Werner: 3.4, 7.7  
Pucher, Andreas: 4.4  
Pynn, Roger: 1.1

## R

Rehm, Christine: 7.14  
Reichert, Harald: 8.1  
Rekveldt, Theo: 1.1  
Rieutord, François: 4.5  
Robinson, Ian K.: 5.1  
Romashev, L.: 2.2  
Ruehm, Adrian: 9.1  
Ruggles, Jeremy L: 11.5  
Ruiz, Ricardo: 7.2  
Rühm, Adrian: 8.3

## S

Saldin, Dilano K.: 12.1  
Salditt, Tim: 9.4  
Sanchez-Hanke, Cecilia: 6.5  
Satija, Sushil: 11.1  
Schlossman, M.: 7.16  
Schmitte, Till: 10.3  
Schreyer, A.: 4.6  
Schuller, Ivan K.: 2.1  
Schüllli, T.: 4.6

Scoles, Giacinto: 7.2  
Seeck, Oliver H.: 7.6, 7.7  
Sellmann, Ralf: 4.3  
Serero, Yaelle: 7.6  
Seydel, Tilo: 8.2, 9.3  
Shih, Ming Chih: 7.12  
Shin, Kwanwoo: 7.12  
Shull, Kenneth: 8.4  
Sinha, Sunil K.: 4.13, 7.11, 7.6, 8.3, 9.1  
Skatkov, Leonid: 4.14  
Smith, Gregory: 11.1  
SNS Instrument Systems Group: 7.13  
Springer, R.W.: 2.1  
Springholz, G.: 4.6  
Sprung, Michael: 3.4  
Srajer, George: 4.2  
Stephens, P. W.: 3.2  
Stephenson, G. Brian: 3.1  
Stetsko, Yuri P.: 7.5  
Stettner, Jochim: 3.4, 7.7  
Streiffer, S. K.: 3.1  
Struth, Bernd: 7.1  
Sztucki, Michael: 5.4

## T

Tang, Mau-Tsu: 7.5  
te Velthuis, S. G. E.: 1.2  
Theis-Bröhl, Katharina: 10.3  
Thiaudiere, Dominique: 4.5  
Thompson, Carol: 3.1  
Tolan, Metin: 3.4, 5.4, 4.10, 7.7, 8.2, 9.3  
Toperverg, B.P.: 2.2, 10.1, 10.4  
Toulemonde, Olivier R. M.: 4.15, 6.3  
Traving, Martin: 3.4

## U

Ustinov, V.: 2.2

## V

van Well, A. A.: 4.8, 4.9  
Vicararo, P.J.: 7.16  
Vlieg, Elias: 11.2

## W

Wagemaker, Marnix: 4.8, 4.9  
Wang, Jin: 7.11, 8.4  
Waring, Alan: 7.4, 8.5  
Weber, Ruediger: 7.7  
Webster, John: 7.3

Weissbach, Danny: 4.10  
Westerholt, Kurt: 7.10  
White, John W: 11.4, 11.5  
White, Robert L: 3.5  
Wolff, Max: 4.12

## Y

Yeh, N.T.: 7.5  
Yu, Kuan-Li: 4.7  
Yacoby, Y.: 3.6

## Z

Zabel, Hartmut: 4.1, 4.11, 4.12, 4.19, 7.10, 10.3  
Zarbaksh, Ali: 7.3  
Zasadzinski, Joseph A.: 7.4  
Zhang, Kai: 11.3  
Zimmermann, Klaus Martin: 4.10